Real-time AI-Assisted Forecasting of Reservoir Capacity Across the United States

Moiyyad Sufi[1], Alejandra Botero-Acosta[2], Carlos E. Ramirez[1], Amanda L. Cox[2], Paul Boyd[3], Marian Muste[4], Ibrahim Demir[1,5]

[1] ByWater Institute, Tulane University, New Orleans, LA
[2] WATER Institute, Saint Louis University, St. Louis, MO
[3] US Army Corps of Engineers, Omaha, NE
[4] IIHR Hydroscience and Engineering, University of Iowa, Iowa City, IA
[5] River-Coastal Science and Engineering, Tulane University, New Orleans, LA

Abstract

Reservoir sedimentation progressively reduces storage capacity, threatening water supply, flood control, hydropower, and ecosystem services across the United States. However, systematic sedimentation monitoring remains sparse, limiting the feasibility of national-scale assessment using traditional methods. This study develops a web-based end-to-end data-driven framework for evaluating reservoir capacity loss across the contiguous United States by integrating historical sedimentation surveys, geospatial feature extraction, and interval-based machine learning. Reservoir sedimentation is formulated as capacity change over time, enabling scalable prediction and cumulative reconstruction of storage trajectories. Results demonstrate reliable performance for medium and large federally managed reservoirs, with predictable limitations outside the training domain. The framework is operationalized through a web-based decision-support application that provides transparent access to model inputs and outputs. This study demonstrates how scalable, data-driven systems can support national prioritization of sedimentation risk and guide strategic reservoir management under limited monitoring conditions.

Keywords: Reservoir sedimentation; reservoir operations; machine learning; geospatial data integration; decision-support systems

Software Availability

Name	RSI Analytics Platform
Cost	Free
Software Required	Web Browser
Program Language	JavaScript, HTML, CSS, Python
Platform Access	https://hydroinformatics.tulane.edu/lab/rsi

This manuscript is an EarthArXiv preprint and has been submitted for possible publication in a peer reviewed journal. Please note that this has not been peer-reviewed before and is currently undergoing peer review for the first time. Subsequent versions of this manuscript may have slightly different content.

1. Introduction

Reservoirs are critical to the United States' water, energy, and environmental systems, yet they face a growing long-term threat from sedimentation and limited monitoring. The nation has around 3.5 million miles of interconnected waterways which support most of the population and reinforce economic and ecological stability (Office of Habitat Conservation, 2026). Within this network, reservoirs provide essential services including water supply, flood control, irrigation, navigation, and hydropower (Annandale et al., 2016). Although only ~5% of U.S. dams are federally owned, they store 61% of national water capacity (Podolak & Doyle, 2015). U.S. water demand approaches 322 billion gallons per day, primarily for thermoelectric power (45%), irrigation (32%), and municipal use (12%) (Hubbart & Ross, 2026). Reservoirs also generate major economic and recreational benefits, supporting over 46 million annual fishing visits and billions in revenue (U.S. Forest Service, 2026), while around 2,700 hydropower facilities produce ~80,000 MW (U.S. Energy Information Administration, 2019).

Despite their importance, reservoirs are steadily losing storage due to sedimentation, i.e. the accumulation of eroded material that reduces capacity over time. A country-wise assessment applying regional sedimentation rates to 47,403 large dams projected a 26% global storage loss by 2050, with the United States among the most affected national portfolios at roughly 10–35%, effectively reverting per capita capacity to mid-20th-century levels (Tullos et al., 2021; Perera et al., 2022). Agency-level accounting reinforces this trajectory. An analysis of 162 USACE reservoirs with sufficient pool volume data found that available water storage in 2024 had fallen back to as-built 1985 level, with the sample losing approximately 210,000 acre-feet per year; and among the 127 reservoirs with at least two surveys, the mean long-term loss rate was found to be 0.45% of initial capacity annually (Shelley & Boyd, 2025).

The impacts are substantial as they include reduced flood storage, impaired hydropower infrastructure, and downstream ecological degradation (Palmieri et al., 2003; Tullos et al., 2021). These risks are intensified by aging infrastructure and changing climate conditions. The average U.S. dam age is 65 years, with many classified as high hazards, with sedimentation compounding structural deterioration in many cases (Perera et al., 2021; Gunderson, 2026). At the same time, increasing hydrologic variability, extreme precipitation, and higher erosion rates are accelerating sedimentation processes (U.S. Army Corps of Engineers, 2026).

Prior national-scale syntheses concluded that U.S. sedimentation management is limited by the sparseness and inconsistency of the survey record (Podolak & Doyle, 2015). National datasets such as the Reservoir Sedimentation Information (RSI) system contains detailed records for only ~400 dams—less than 1% of the over 90,000 in the U.S. (U.S. Army Corps of Engineers, 2015; Cox et al., 2024). These data are also temporally sparse, with many reservoirs lacking updated surveys for decades due to funding limitations (Pinson et. al., 2016). Physical sediment transport models such as HEC-RAS resolve sediment transport in detail but require dense geometry, boundary condition and calibration data which is far sparser at national scale (Gibson & Sánchez, 2020; Li, H., et al., 2022).

Traditional empirical approaches are similarly insufficient. Brune's trap-efficiency curve (Brune, 1953) applies only to long-term average conditions, and Brune noted that significant departures occur when operating rules change; trapping also depends on the pool level actually held during floods and on outlet placement and which the capacity-to-inflow ratio does not capture. As a result, current approaches cannot reliably support long-term planning. A critical

gap exists between sparse observational data and the need for scalable, predictive tools, highlighting the need for advanced data-driven methods in hydroinformatics systems (Yesilkoy et al., 2024), which can be applied to assess sedimentation across thousands of unmonitored reservoirs.

This study focuses on the development and validation of a scalable, data-driven methodology capable of forecasting reservoir sedimentation across the contiguous United States operationalized through a web application that contains reservoirs from around the US and provides a data driven assessment of pool evolution using deep learning techniques. The specific objectives defining the scope of this study are:

a) Development of a national-scale reservoir sedimentation assessment framework: Formulate a generalized approach for modeling U.S. reservoir capacity by synthesizing high-resolution, nationwide geospatial parameters (including precipitation intensity, watershed topography, and soil characteristics) with reservoir construction data (upstream dam storage and height, and initial reservoir capacity).
b) Implement a web-based decision-support application: Ensure the immediate translational impact of the predictive model by integrating their outputs into an accessible, web-based decision-support system (DSS), enabling stakeholders to visualize regional reservoir capacity status.
c) Evaluate the predictions of the application: Evaluate the predicted capacity loss results by comparing them with a limited survey capacity dataset and discuss comparison results based on the selection of reference records and the modelling methodology.

This manuscript is organized as follows. Section 2 provides background on reservoir sedimentation processes, existing assessment approaches, national monitoring efforts in the United States, and recent applications of machine learning in sediment and hydrologic modelling. Section 3 describes the methodology, including development of supplemental geospatial and climatic variables associated with reservoirs, the machine-learning framework, the deployment of the predictive system through a web-based application, and the characterization of the US reservoir dataset used as benchmark. Section 4 presents the results, including the characteristics of the curated national reservoir dataset and demonstration of model outputs through regional case studies. Section 5 discusses the scientific contributions, implications for reservoir management, inherent limitations of the approach, and directions for future research. Section 6 concludes with a summary of key findings and the role of scalable, data-driven tools in supporting long-term reservoir sedimentation assessment and water resources management.

2. Background

2.1. Reservoir Sedimentation Processes and Impacts

Reservoir sedimentation is fundamentally governed by sediment mechanics in upstream, the reservoir impoundment and downstream zones (Whelan & Hotchkiss, 2024). Recent reviews synthesize these mechanics through processes like delta progradation, density-current propagation, consolidation of fine deposits; along with the management responses available at each stage (Sohrabzadeh Anzani et al., 2026; Schleiss et al., 2016). The process initiates with sediment generation within the watershed, where rainfall erosivity and land-use change detach soil and deliver sediment into the riverine network (Mouris et al., 2023). As these sediment-

laden flows enter the reservoir, the sudden expansion of cross-sectional area and sharp reduction in flow velocity trigger deposition of suspended and bed-load sediments. Deposition follows a consistent sequence. Coarser sand and gravel settle near the reservoir inlet, forming a delta with top-set, fore-set, and bottom-set regions (Morris & Fan, 1998; Schleiss et al., 2016). Silt and clay remain in suspension far longer and travel deeper into the impoundment. Sediment held in suspension by flow turbulence forms a two-phase mixture denser than the ambient water, which plunges beneath the clear water as a turbidity current (Fan, 1986; Schleiss et al., 2016). These currents follow the submerged topography of the basin and carry fine sediment toward the dam, where deposition can form a muddy layer near the dam face.

The impacts of this sediment deposition extend beyond storage loss. Sedimentation alters the sediment regime and changes substrate composition in the reservoir and downstream, with consequences for aquatic organisms that have specific substrate requirements (Juracek, 2015). These changes compound the loss of river connectivity alongside fragmentation and flow regulation (Grill et al., 2019). The time scales of sedimentation conflict with historical engineering paradigms. Reservoirs in the United States were generally sized to store sediment during a design life of 50 or 100 years before deposits encroach on the lowest dam outlet (Randle et al., 2021).

This approach ignored the consequences of continuing sedimentation beyond the original design life. Loss rates vary sharply by region: average life expectancy for surveyed reservoirs in the interior west was under 100 years vs. more than 300 years in parts of the East (Graf et al., 2010). Allowing sedimentation is unsustainable and requires a shift from design life to sustainable use, balancing sediment inflow and outflow (Randle et al., 2021). Techniques for lifecycle management like bypass, sluicing, and drawdown flushing are documented worldwide (Kondolf et al., 2014) and, within the United States. These techniques, in some cases, have been shown to work cost-effectively and within existing permitting requirements (Shelley et al., 2022).

2.2. Existing Approaches to Reservoir Sedimentation Assessment

Historically, reservoir sedimentation has been assessed using empirical sediment yield models and trap efficiency (TE) curves, which estimate the fraction of incoming sediment retained in a reservoir. Foundational approaches such as Brune (1953) and Churchill (1948) relate trap efficiency to the capacity-to-inflow (C/I) ratio, assuming reservoirs with larger storage relative to inflow retain more sediment. However, these methods often overestimate trap efficiency in shallow or irregular reservoirs due to missing flow patterns or secondary currents, or with high in-flow variability during floods (Sohrabzadeh Anzani et al., 2026).

Empirical methods also predict only the shift in the stage-area and stage-capacity curves without identifying where deposition occurs, and they cannot simulate the effect of a change in scenario such as introducing sediment management (Morris & Fan, 1998). Efforts to place these empirical relations on a broader observational footing have accelerated with the release of curated, open sedimentation archives, though the underlying sparseness across physiographic regions remains large (Minocha & Hossain, 2025).

Physically based models, such as HEC-RAS, offer more rigorous, process-based simulations using sediment transport equations like Meyer-Peter Müller (Gibson & Sánchez, 2020). These models are strongly data-dependent and require adequate data for calibration and

verification, which, in practice, is often lacking, and two independent datasets for formal verification are frequently unavailable (Morris & Fan, 1998). Extending such models to continental domains requires substantial simplification of transport physics and remains sensitive to poorly constrained hillslope-erosion and channel-storage parameterizations (Li, H., et al., 2022; Mouris et al., 2023). As a result, applying these models across large, heterogeneous watersheds is computationally intensive and highly uncertain, limiting their scalability to national assessments.

This challenge mirrors findings in adjacent hydroinformatics domains. Culvert sedimentation cannot be readily addressed by conventional analytical modeling approaches because the problem involves complex and interlinked environmental processes, so Xu et al. (2019) instead identifies factors involved in sedimentation drivers from multi-disciplinary data through a web-based platform. The same logic scales globally: RECLAIM couples 88 static and dynamic catchment, climatic, and reservoir-specific features with satellite observations from 1984 to 2023 across 1,315 observations from 984 reservoirs, using a dynamic ensemble of gradient boosting models to predict absolute sedimentation rate (Minocha et al., 2026). Furthermore, anomaly detection methods have proven essential for scrubbing historical multi-agency reservoir survey databases to enable reliable multivariate predictive modeling (Botero-Acosta et al., 2024; Cox et al., 2024).

Similarly, open-source initiatives underscore the need for platforms that aggregate data and unify their format for building these kinds of models. The River Morphology Information System (RIMORPHIS) exemplifies this by providing a web-based cyberinfrastructure built on NHDPlus HR that aggregates, visualizes, and analyzes river morphology data, including sedimentation and roughness measurements (Sermet et al., 2025). Aggregating different data sources raises a semantic problem as well as a coverage problem: hydrological data are heterogeneous, disorganized, and non-interoperable, which limits decision makers' access to the information they need (Baydaroğlu et al., 2023).

Advances in computational power, high-resolution geospatial data, and artificial intelligence have driven rapid growth in applying Machine Learning (ML) to hydrology and water resources (García-Feal et al., 2022; Granata et al., 2022; Demiray et al., 2024). Reviews of trends in hydrological analysis position this growth within a broader methodological transition, emphasizing that predictive skill in sparse-data settings is bounded less by model capacity than by the information content of the observational record. A key advantage of these approaches is their ability to capture complex, nonlinear relationships across diverse datasets without requiring explicit physical parameterization.

Recent studies show that ML models outperform traditional methods in sediment yield forecasting, with hybrid models achieving high-fidelity tracking in localized systems (El Bilali et al., 2024). While techniques such as Generalized Linear Models, Random Forests and Gradient Boosting methods have been used, earlier efforts often lacked deeper optimization of model architectures. Scaling these approaches to assess reservoir capacity loss across the United States requires models capable of integrating complex, multi-dimensional datasets, as simpler ML models often struggle to capture large-scale sediment dynamics (Cox et al., 2024).

2.3. National Reservoir Monitoring in the United States

Large-scale sedimentation assessment depends on robust, standardized monitoring data. In the United States, reservoir surveillance is primarily conducted by the U.S. Army Corps of Engineers (USACE) and the Bureau of Reclamation (USBR). Historically, their data were housed in the Reservoir Sedimentation Survey Information System (RESIS) Database (Steffen, 1996). The immediate predecessor to these holdings is the Reservoir Sedimentation Survey Information System, whose second release (RESIS-II) reorganized and quality-checked digitized survey records and remains the primary source of historical capacity measurements used in U.S. analyses (Ackerman et al., 2009).

This database was revised and supplemented by the U.S. Geological Survey (USGS), Advisory Committee on Water Information, Subcommittee on Sedimentation to develop the Reservoir Sedimentation Database (RESSED) (Advisory Committee on Water Information, 2009). Finally, the USACE led an interagency effort to develop Reservoir Sedimentation Information (RSI) web portal to archive surveys, standardize reporting, and create a centralized platform that links historical surveys with other federal databases and supports interactive, web-based analytics (U.S. Army Corps of Engineers, 2015).

It is also worth noting that temporal coverage is uneven. USACE guidance recommends resurveys every 5 to 10 years, but budget limitations often prevent surveys at that interval; among six districts assessed, several reservoirs had gone more than 30 years without a survey and others had never been surveyed since closure (Pinson et al., 2016). USACE attributes this to O&M budget constraints that have limited periodic sediment surveys (U.S. Army Corps of Engineers, 2026). As a result, analyses rely on sparse, outdated data, underscoring the need for advanced methods to estimate current and future conditions (Randle et al., 2021). Integrating information-centric flood ontologies directly into these management practices would facilitate semantic data harmonization (Baydaroğlu et al., 2023).

Finally, the National Inventory of Dams (NID) (USACE, 2021) is a database maintained by the U.S. Army Corps of Engineers containing general information on more than 90,000 structures across the U.S., including dam location, characteristics at construction, purpose, and hazard classification. Although this dataset does not contain survey information, it includes reservoir storage and dam height at the time of construction.

2.4. Web-Based Hydroinformatics and Digital Twins

The operationalization of these advanced machine learning models requires an equally advanced web-based cyberinfrastructure. Hydroinformatics has rapidly evolved from monolithic, highly localized server-side architectures to distributed, client-side web applications that leverage standard web browsers for complex geoprocessing, visualization, and user interaction. Early platforms addressed the hurdles that deter environmental web app development by, for example, bundling open-source geospatial software with a Python development kit and a deployment portal (Swain et al., 2016). Browser-side computation followed, with terrain-derived hydraulic models such as Height Above Nearest Drainage implemented and evaluated directly in the browser against operational national implementations (Li et al., 2023). The trajectory now extends to digital twins that integrate flood forecasting, transportation networks, and critical infrastructure, addressing the inability

of conventional mapping tools to incorporate real-time data or analyze cascading disruptions across interconnected urban systems (Kaynak et al., 2025; Beck et al., 2010).

Open-source frameworks have lowered the barrier to browser-based hydrological computing. Modular client-side web components now support data acquisition, management, and visualization within the browser (Erazo Ramirez et al., 2023), extended to comprehensive flood risk communication (Sufi et al., 2025). Recent progress has even extended to client-side web-based model coupling, linking hydrological models through standardized basic model interfaces (Ewing et al., 2024). These interactive web-based decision support systems (DSS) have proven effective in incorporating user-friendly applications to demonstrate algorithms and methods in an intuitive manner to improve scenario-based decision making (Alabbad et al., 2024; Demir & Beck, 2009).

Building on these developments, the following methodology operationalizes a scalable framework that integrates heterogeneous national datasets within a unified modelling pipeline, leveraging recent advances in deep learning and web-based hydroinformatics to enable consistent, large-scale estimation of reservoir sedimentation and capacity loss.

3. Methodology

3.1. Machine Learning Framework

We employed a deep neural network (DNN) to predict the reservoir capacity loss for selected RSI reservoirs with more than one survey as described in Cox et al., 2024. The training and testing dataset for DNN was created by compiling reservoirs and associated basins information from the RSI and publicly available datasets. The prediction target was the change in RSI reservoir storage capacity (in acre-feet) over a discrete time interval between surveys, defined as Eq.1. Capacity changes were estimated as the difference in reservoir's capacity at the maximum pool elevation between two consecutive RSI surveys, excluding elevations designated as the surcharge pool. Differences between the selected pool elevation and those reported in other USACE documentation may occur due to variations in pool-naming conventions or discrepancies associated with manual data entry and verification.

$$\text{Capacity Change} = \text{Capacity at start of interval} - \text{Capacity at end of interval} \quad \text{Eq. 1}$$

A positive value would indicate a net capacity loss due to sediment accumulation; a negative value indicates capacity gain (e.g., from dredging or measurement variation). Given that the DNN was developed to reproduce sedimentation processes rather than sediment management measures, only records with capacity loss between RSI surveys were included in the training and testing dataset. The input features consisted of 12 predictor variables per observation as listed in Table 1. These could be classified as three climatic (mean, maximum, and cumulative precipitation), six geomorphic (basin area, centroid latitude, hydraulic length, basin relief, channel slope, and curve number), two infrastructure (upstream dam storage and upstream dam height), and one reservoir characteristic (initial capacity). Predictor variables for the DNN training and testing dataset were developed using the same sources specified in Table 1 for the WebApp, except for the Initial Capacity, which was obtained from the RSI dataset. This formulation treated each consecutive RSI survey pair as one labelled training observation, where the target was the observed capacity loss between surveys, and the input features

characterized the reservoir, associated watershed, and climatic conditions over that time interval. This target variable ensured that prediction errors did not compound unboundedly and that the model generalized across reservoirs with different ages and initial sizes.

Before training, the target variable and all input features were passed through a signed log transform to compress the wide dynamic range of values (spanning several orders of magnitude) while preserving the sign of directional changes (Eq. 2). A min-max scaling ranging from 0.15 to 0.85 was then implemented to normalize the input variables to a common range, preventing differences in variable magnitude from disproportionately influencing model training, and a zero centering was applied on the data. Finally, a Principal Component (PC) transformation was performed to reduce dimensionality and improve computational efficiency.

$$x_{transformed} = \text{sign}(x) * \log(|x|) \quad \text{Eq. 2}$$

The model architecture was formulated as a fully connected deep neural network with 13 layers of trainable weights. Regularization was applied after the 256-unit and 1024-unit blocks, each consisting of a Batch Normalization layer followed by a Dropout layer with a rate of 0.3. The output layer used a linear activation function, appropriate for the continuous regression target. This architecture is shown in Figure 1. The pipeline fitted on the training data and serialized; at inference time the same fitted pipeline would be loaded and applied to new inputs before they are passed to the model, which would return a predicted capacity loss for the corresponding time interval.

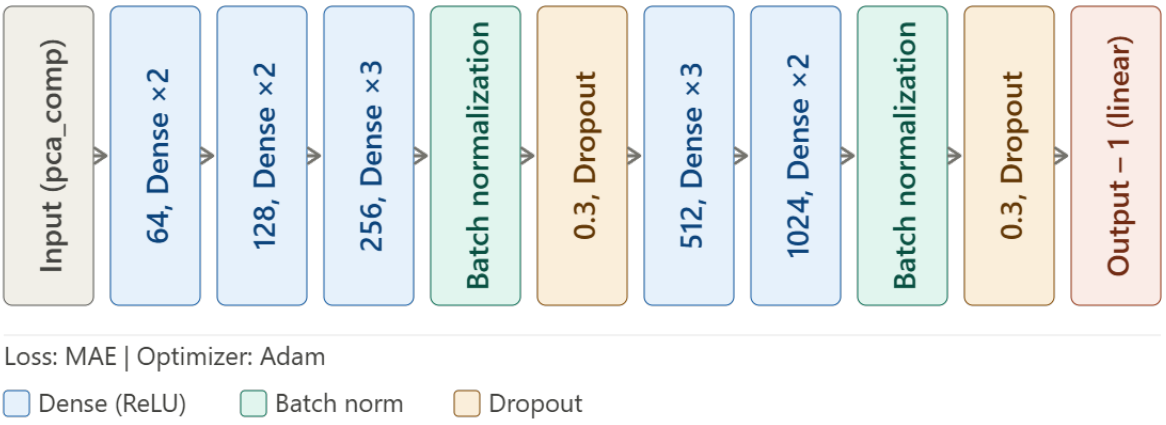


Figure 1. Architecture of the deep neural network used to train and infer reservoir capacity loss over time, adopted from Cox et al., 2024.

3.2. Web Application Development

To formulate a generalized approach for modeling reservoir capacity across U.S., the trained DNN model was applied to the broader NID reservoir dataset with limited survey data. An interval-based target decomposes the problem into shorter, more stationary windows instead of predicting absolute capacity at a point in time, which would require the model to learn the full history of a reservoir. Time intervals were defined as 15-year windows from a reservoir's completion year to the present. As a result, a time series of reservoir's capacity was reconstructed cumulatively at inference time by subtracting successive DNN predicted losses

from the initial NID capacity. For this, the reservoir and associated basin parameters data were obtained from publicly available sources (Table 1) and passed to the DNN to predict the capacity losses for the corresponding 15-year time step.

Shapefiles of reservoirs' associated basins were used to extract geospatial data from upstream drainage areas. Basin delineation was performed using python scripts that accessed two main databases: NHDPlus database (EPA, 2022), developed and maintained by USGS and EPA, and accessed via the PyNHD data retriever package (Chegini et al., 2021), and Merit-Hydro database (Lin et al., 2019; Yamazaki et al., 2019), analyzed using modified code based on Heberger (2023). Areas of resulting delineated polygons were compared with reported NID drainage areas, only reservoirs for which the delineated basin area closely match NID values with less than 10% error were kept. Consequently, NID reservoirs lacking either initial capacity value or an associated basin shapefile were excluded from the analysis.

Table 1. Summary of variables employed in the WebApp.

Variable	**Units**	**Temporal Nature**	**Variable Type**	**Source for WebApp Implementation**
Mean monthly precipitation	in/mo	Time-dependent	Observed	PRISM via Google Earth Engine
Maximum monthly precipitation	in	Time-dependent	Observed	PRISM via Google Earth Engine
Cumulative precipitation	in	Time-dependent	Observed	PRISM via Google Earth Engine
Upstream dam storage	ac-ft	Time-dependent	Observed	NID inventory shapefile
Upstream dam height	ft	Time-dependent	Observed	NID inventory shapefile
Basin area	mi^2	Static	Derived	Watershed delineation (MERIT / USGS NLDI)
Centroid latitude	deg	Static	Derived	Watershed polygon centroid
Hydraulic length	ft	Static	Derived	MERIT-Hydro flow direction rasters
Basin relief	ft	Static	Derived	USGS 3DEP DEM via Google Earth Engine
Channel slope	-	Static	Derived	Derived (relief / hydraulic length)
Curve number	-	Static	Derived	NLCD land cover + NRCS soil groups
Initial capacity	ac-ft	Static	Observed	NID database (Normal or Max Storage)

The predictive model was deployed as an interactive web application called RSI Analytics Platform built with an architecture comprising of a browser-based client, a Python application server, and a layer of local and external data infrastructure. The full system is illustrated in Figure 2. The client-side runs entirely within a standard web browser and consists of several functional components. The primary interface is a Google Map and HTML interface through which the user can interact with the application. Alongside the map, a supplementary data collection wizard guides the user sequentially through watershed delineation, static feature

review, climate and infrastructure data retrieval, and final forecast generation. A client and server-side caching layer stores processed information so that retrieval of existing run dams is more performant. An administrative interface provides access to the server-side delineation cache, allowing inspection, deletion, and bulk clearing of cached site records. The application server is implemented in Python using Flask and Flask-SocketIO, with all logic contained on the server-side application module that imports processing functions from a structured code base. Concurrency is managed through per-site threading locks that prevent duplicate delineation jobs for the same location from executing simultaneously across sessions.

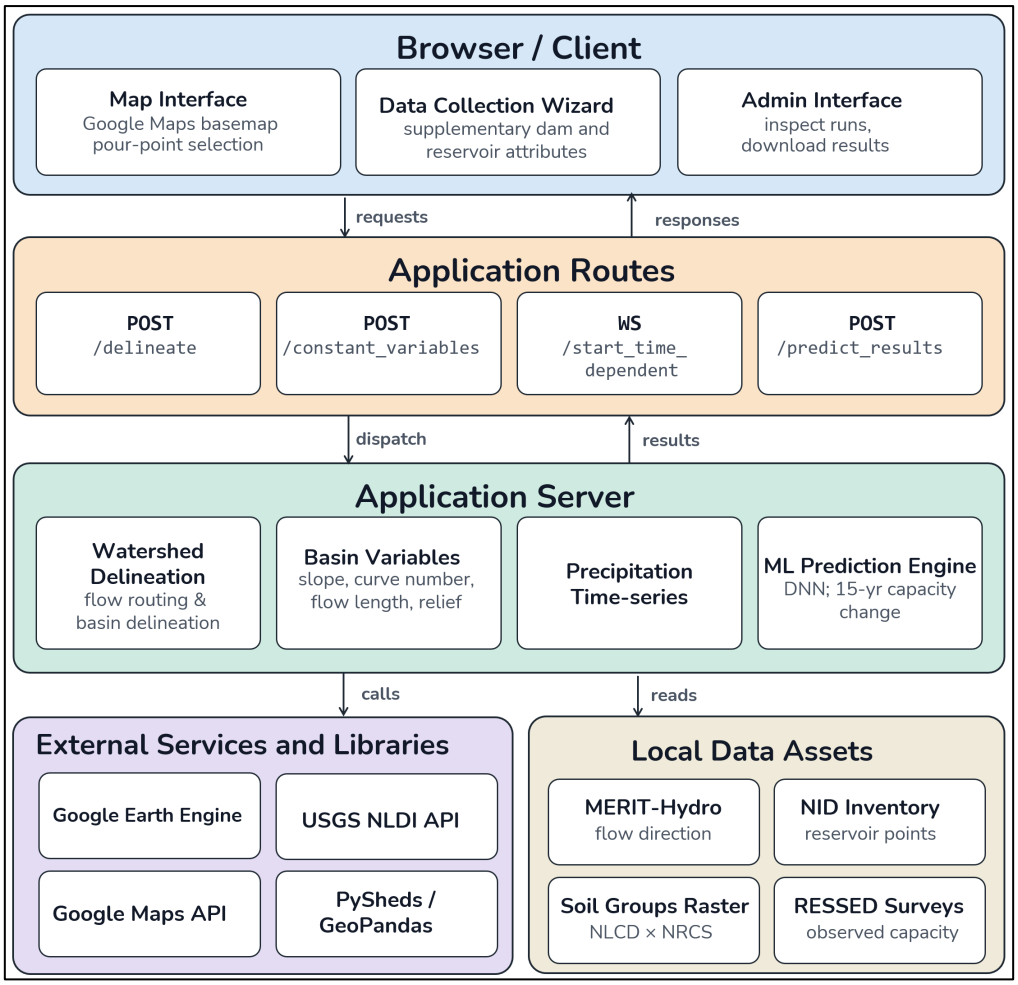


Figure 2. System Architecture Diagram for Reservoir Sedimentation Information App.

The end-to-end computational workflow from dam selection to sedimentation forecast is organized as a four-phase sequence, illustrated in Figure 3. Following reservoir identification through the map interface or NID-based search, the workflow enters the first phase, in which the upstream watershed associated with the selected dam is delineated. This phase establishes the spatial domain required for all basin scale computations and concludes with the presentation of the generated watershed boundary within the client interface, along with diagnostic information that supports verification of the delineation outcome.

The second phase focuses on basin characterization. Once the watershed geometry has been finalized, a set of static geomorphic and reservoir attributes is computed and returned to the

client. These quantities describe constant basin and storage properties and are retained for the duration of the analysis. Exposing these values at this stage allows users to review foundational inputs before time-dependent processing begins. In the third phase, the application assembles time-dependent predictors across successive pre-defined time intervals beginning at the dam completion year. Precipitation-related variables and upstream infrastructure metrics are computed sequentially on the server for each time interval. The data is processed in 15-year intervals from the dam completion date to the present. For each interval the system first queries the PRISM AN81m monthly precipitation dataset through Google Earth Engine, computing the spatial mean precipitation over the watershed polygon for every calendar month in the interval and deriving mean monthly, maximum monthly, and cumulative precipitation in inches. Then, the NID inventory shapefile is used to identify all dams located within the watershed polygon that were completed before the end of the interval, computing the cumulative normal storage, or maximum storage when unavailable, and cumulative dam height of those upstream structures averaged across the years in the interval. Because this phase involves the largest computational requirement, progress indicators are provided to communicate execution status and maintain continuity between user interaction and background processing. Supporting tables summarizing basin attributes and interval-level drivers remain accessible alongside the visualization, reinforcing transparency in how predictions are produced.

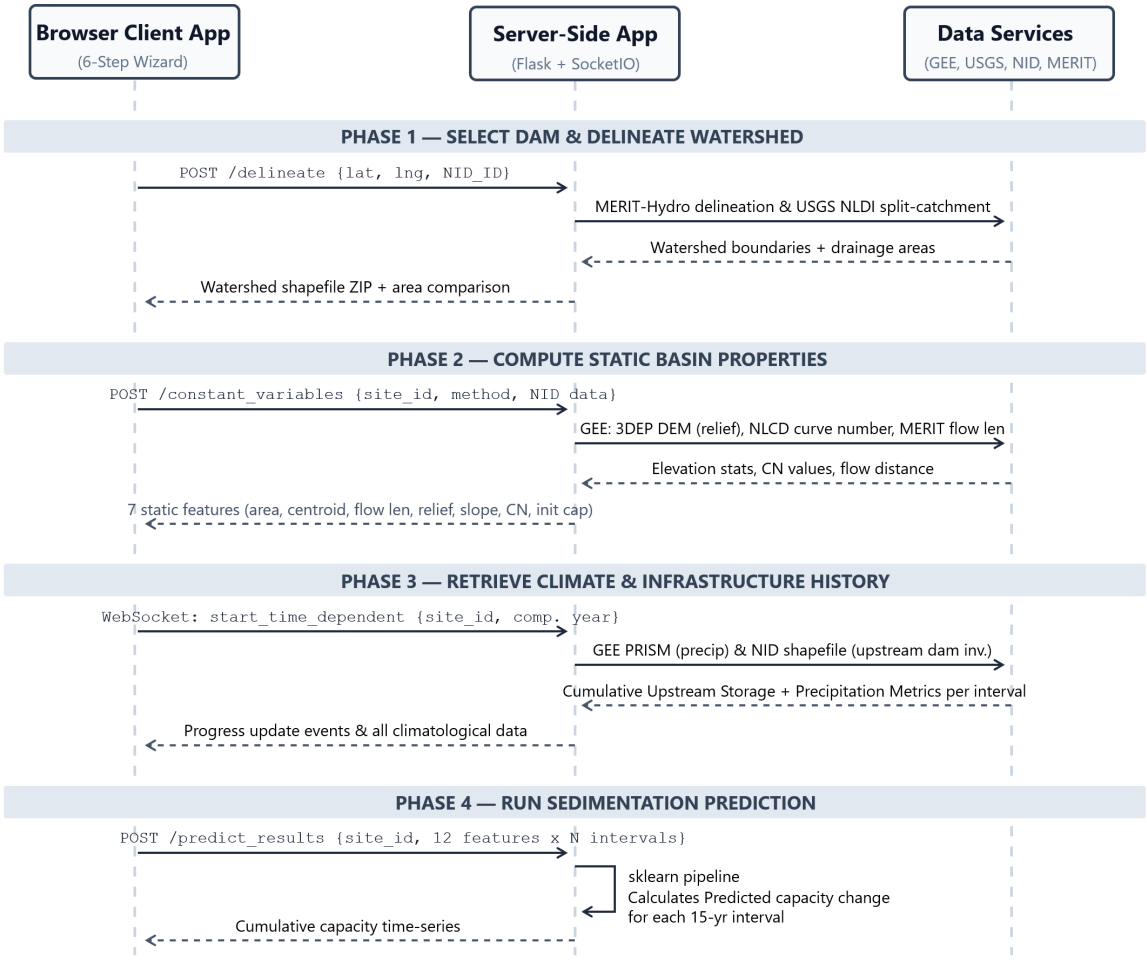


Figure 3. Sequence diagram showing distinct steps for data collection and model inference to predict capacity loss over time.

The fourth phase executes model inference. The complete 12-feature predictor matrix for each 15-year interval is transformed using the fitted preprocessing pipeline before passing it to the DNN. This consists of applying the log transformation to all features, then passing them through a min-max scaler ranging from 0.15 to 0.85 and finally executing the PC transformation. Results from the DNN would correspond to the predicted capacity loss in acre-feet for each interval. These changes are accumulated from the initial NID capacity to produce a complete time series of predicted reservoir storage capacities, beginning at the completion year and extending to the present. The resulting time series is rendered as an interactive visualization that depicts long-term capacity evolution from dam commissioning to the present.

3.3. Web Application Validation

Publicly available reservoir capacity survey data from federal agencies, compiled in the RESSED database, were used to develop a benchmark dataset for validating reservoir capacity losses simulated by the application. Establishing robust benchmark datasets is crucial in machine learning, as they serve as the foundation for scientific reproducibility and enable standardized, transparent model evaluation (Ebert-Uphoff et al., 2017). For this, an observational baseline dataset of measured storage-capacity changes in storage capacity was assembled for a nationally distributed set of dams. For selected reservoirs with survey-based capacity data covering the simulation period, the observed capacity losses were compared with the simulated values to provide observational context, and validation metrics were calculated.

3.3.1. Benchmark Dataset

The benchmark dataset was created from reservoir capacity data obtained from the RESSED database, a federal repository maintained by the USGS Subcommittee on Sedimentation that compiles historical bathymetric and sedimentation survey records for dams across the nation managed by multiple agencies and encompasses structures of varying sizes and capacities. Each RESSED survey provides a measured pool capacity (in acre-feet) and, in most cases, a surface area (in acres) at the time of the survey.

Survey data were organized by reservoir identifier, geographic location, and survey date. Records for reservoirs missing NID IDs, initial NID storage, completion year or outside the contiguous United States were removed. Records which had their survey date was before the NID completion date for the respective reservoir also not included. In cases where there were more than one survey of the same storage pool in a calendar year for a reservoir, the earliest record in that year was retained.

Each RESSED record holds one capacity value for one storage pool on one survey date, identified by a single-letter designation: T, S, A, or G, with some undesignated records. These designations are listed in the RESSED documentation without further definition, and the survey table (RSED04) and the pool table (RSED02) follow different pool naming systems (Ackerman et al., 2009). In RSED02 table, the original storage is divided by purpose into flood control, multiple use, power, water supply, irrigation, conservation, and inactive pools. Each survey designation was interpreted by comparing its first chronological T capacity record (T0) capacity, with the RSED02 pool capacities for each reservoir. As a result, T was identified as the capacity through to the flood control pool and to the elevation of the topmost spillway total-pool capacity. Survey records with pool elevation values marked with T, were retained to be

used in benchmarking dataset creation, with T0 a uniform measure for the initial RESSED capacity of the reservoirs.

To be able to estimate capacity loss values between two subsequent surveys, only those reservoirs with two or more surveys were kept. Due to differing conventions in completion dates and dates when the reservoir began regular operations, many reservoirs had differing RESSED and NID completion dates. To resolve this, reservoirs with at least one survey within 5 years after NID completion year were kept and rest were dropped, allowing a uniform ground to compare the NID and RESSED capacities, described in subsequent steps. Additionally, observed changes in reservoir's capacity were calculated by pairing consecutive surveys and computing the difference in reported storage over the intervening period. Under normal sedimentation processes, reservoir storage capacity is expected to decrease monotonically over time. However, capacity increases may reflect dredging, dam raises, measurement inconsistencies between survey methods, or changes in reference pool elevation. Because these factors cannot be reproduced by the DNN, these records were dropped.

The NID initial storage values were then compared to the first survey and only reservoirs for which the capacity value reported in the RESSED initial survey and the NID initial capacity agreed within 10% were included in the benchmark dataset. This, ensured a consistent baseline for comparing modeled and observed capacity losses.

3.3.2. Validation Metrics

The Web Application results were compared with the benchmarking dataset. Validation metrics were used to quantify the agreement of observed and simulated capacity values, which we define in this section. As the WebApp reported reservoir capacities in 15-year increments starting from NID completion date, we used linear interpolation (Eq.3) to create a yearly time series of predicted reservoir capacities to align simulated and benchmarking years.

$$\hat{F}(t) = \hat{F}_{k-1} + \frac{t - t_{k-1}}{t_k - t_{k-1}}\left(\hat{F}_k - \hat{F}_{k-1}\right), \quad t_{k-1} \le t \le t_k \qquad \text{Eq. 3}$$

where $\hat{F}_k$ is the predicted capacity at the end of the period k. With $\hat{F}_0$ being the original NID Storage at the NID completion year t_0. Following this setup, we can calculate a set of metrics to evaluate model results.

Absolute error: This metric was used to compare the absolute difference between simulated capacity $\hat{F}_i$ and observed capacity F_i from survey taken in year t_i. Absolute error values have the same units as the observed data, allowing for an intuitive interpretation of the computed difference in absolute terms, with a zero-value indicating a perfect model (Dawson et al., 2010).

$$Absolute\ error\ (|\ e_i\ |)\ = |\,\widehat{F}_i - F_i|, i = 1,2,3\ldots \qquad \text{Eq. 4}$$

Mean absolute percentage error (MAPE): This metric measures the average error as a percentage of the surveyed capacity. Normalized values allow result comparison for reservoirs of different sizes:

$$\text{MAPE} = \frac{1}{n}\sum_{i=1}^{n}\frac{|e_i|}{F_i} \times 100 \qquad \text{Eq. 5}$$

This metric is suitable for datasets with a limited number of observed records. Moreover, because it expresses errors as percentages, it enables comparisons between larger and smaller reservoirs on a common scale (Hodson, 2022).

Percentage Bias: This metric estimates the cumulative error between predicted and surveyed capacities normalized by the sum of surveyed capacities and could vary from -Infinity to Infinity, with 0 being the optimal value, indicating no bias. It shows the overall direction of the model's error: a positive PBIAS indicates that the model predicts larger capacity values than the surveyed ones, while a negative PBIAS means it under-predicts capacity values. This metric has been used in hydrological analysis with examples in Alfieri et al., 2014 and Gupta et al. 1999.

$$\text{PBIAS} = 100 \times \frac{\sum_{i=1}^{n}\left(\widehat{F}_i - F_i\right)}{\sum_{i=1}^{n}(F_i)} \qquad \text{Eq. 6}$$

Comparing the PBIAS value with MAPE can reveal systematic errors for a reservoir, as PBIAS keeps the sign of the error, while MAPE does not. When the two are similar in magnitude, the predicted capacity is above or below every survey by a similar amount. This results from an initial offset (Eq. 7) or from a steady under- or over-prediction of loss. When PBIAS is much smaller in magnitude than MAPE, the predicted capacity is above some surveys and below others, and the predicted rate of loss differs from the surveyed rate.

Initial Offset: A source of error in this analysis is the difference between the NID storage used to start the simulation and the capacity in the first retained survey. The two records can refer to different survey conventions, and the benchmark dataset only limits this difference to 10%. The initial offset is calculated as a percentage of the surveyed capacity:

$$\text{Initial offset} = \frac{F_0 - F_{i=1}}{F_{i=1}} \times 100 \qquad \text{Eq. 7}$$

where F_0 is the NID storage at the NID completion year t_0, and $F_{i=1}$ is the capacity from the first RESSED retained survey. A positive value means the simulation time series starts above the surveyed capacity, and a negative value means it starts below.

4. Results

4.1. Web Application

The primary user input is the identification of a target dam, either by name or ID search within the NID inventory or by selection of a dam on a Google Map interface. The dams available for

selection are from the NID inventory data as shown in Figure 4. Once a dam is selected the watershed can be generated and viewed on the Google Maps interface.

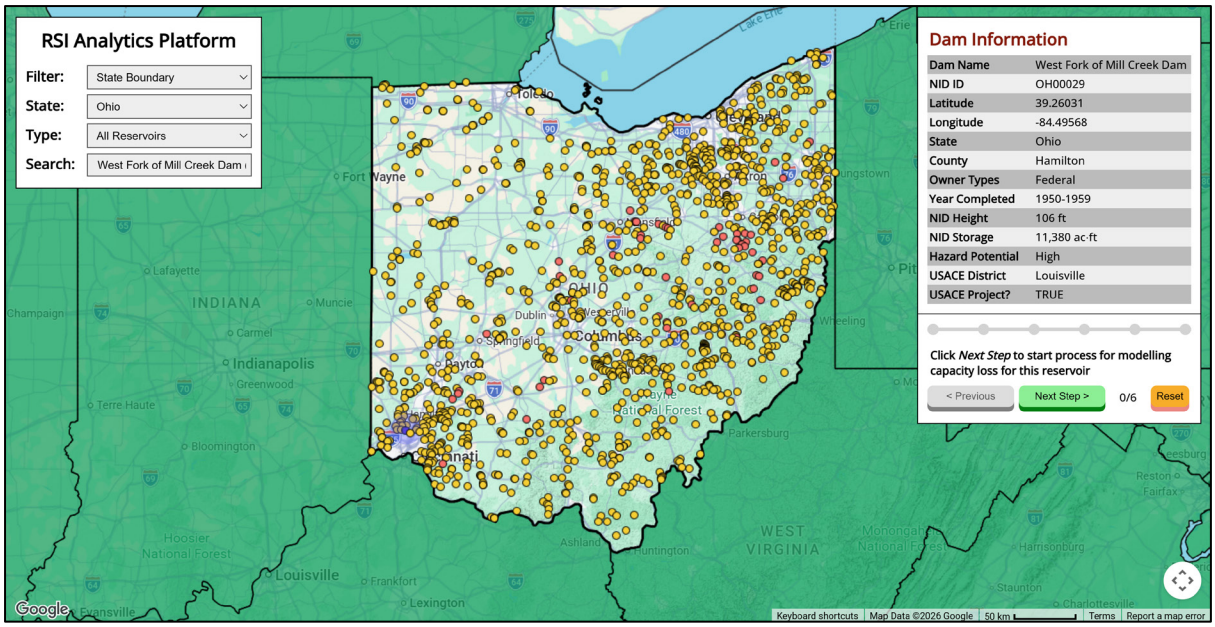


Figure 4. RSI interface showing all available reservoirs filtered by Ohio State. West Fork of Mill Creek Dam is shown to be selected on the interface.

Intermediate outputs are surfaced to the user at each wizard step, providing transparency into the quantities that drive the prediction. After delineation, the watershed polygon is rendered as a vector overlay on the Google Maps basemap alongside a numeric comparison of the delineated area versus the NID-reported drainage area, indicating which method was selected and by what margin. After static feature computation, the six geomorphic variables are displayed in a tabular review panel so the user can inspect basin latitude, hydraulic length, relief, slope, curve number, and initial storage before proceeding. After the time-dependent phase, the upstream dam history is presented as a per-interval summary showing cumulative upstream storage and dam height alongside the precipitation statistics for each 15-year window, allowing the user to contextualize the hydrologic and infrastructure conditions that the model will use for each prediction interval.

An example of the workflow is shown in Figure 5 for Mill Creek Dam, OH. Real-time feedback during the computationally intensive time-dependent phase is provided through Socket.IO. The app tracks progress events as each 15-year interval are processed. The final prediction output is rendered as a capacity loss chart displaying predicted reservoir storage in acre-feet as a function of time from the dam's completion year to the present. The chart is produced using the Google Charts library and plots the cumulative capacity trajectory, optional observed RESSED survey values, alongside horizontal reference lines at the initial NID storage value. This result is shown in Figure 6 and 7.

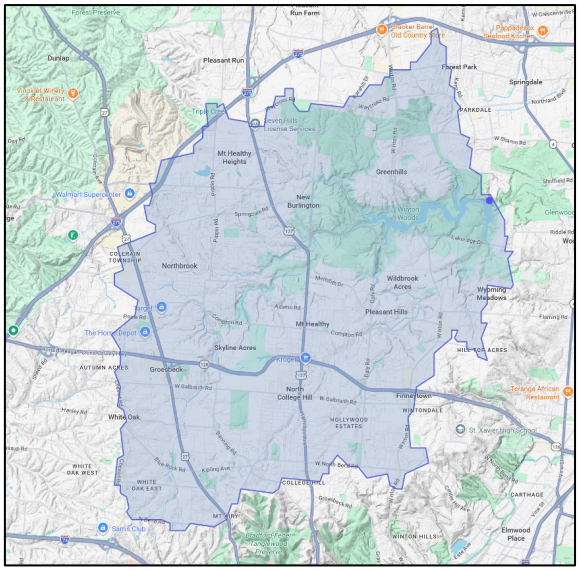


Figure 5. Zoomed in view of the watershed generated for Mill Creek Dam using the MERIT method.

Avg. Basin Latitude	39.24	More
Basin Relief	296 ft	

Hydraulic Length	68,805.09 ft	More
Channel Slope	<0.01	
Curve Number (CN)	70	
Initial Capacity	11,380.00 ac-ft	

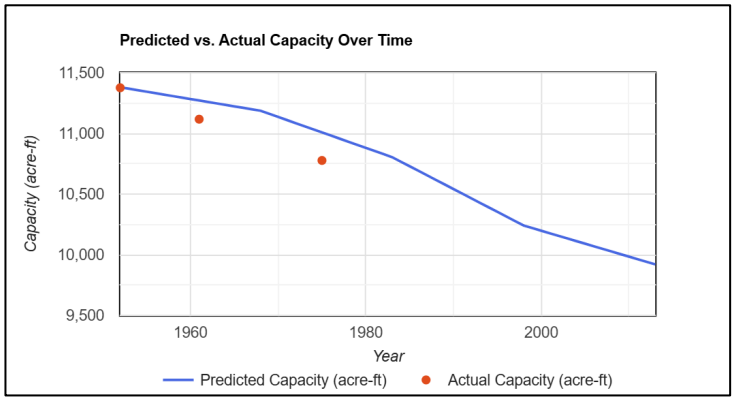
Start Year	End Year	Cumulative Rain (in)	Max Monthly Rain (in)	Mean Monthly Rain (in)
1953	1968	570.02	10.52	3.17
1968	1983	618.15	10.21	3.43
1983	1998	623.81	11.03	3.47
1998	2013	668.78	13.31	3.72

Click *Next Step* to view Upstream Data

Start Year	End Year	Dam Height (ft)	Max Storage (Ac-ft)	Normal Storage (Ac-ft)
1953	1968	0.00	11380.00	1530.00
1968	1983	0.00	11380.00	1530.00
1983	1998	24.20	11553.65	1658.77
1998	2013	104.50	12217.20	2152.40

Click *Next Step* to view Time Series Capacity Loss Data

Figure 6. Results for output results for static and time dependent variables for model inference.



% Loss (1952 - 2013)	12.8%
Avg. Yearly Loss	0.21% / yr
Model Error (RMSE)	160 ac-ft

Figure 7. Final capacity loss shown over time for Mill Creek, OH. The Dam is predicted to lose around 13% of its capacity in the period 1952 to 2013. There are three RESSED surveys available for this location, which yields an RMSE value of 160 ac-ft for our model.

4.2. Web Application Validation

4.2.1. Benchmark Dataset

RESSED dataset contains data from ten reporting agencies, and the composition is dominated by small watershed structures: 1,211 of the 1,823 reservoirs were surveyed under Soil Conservation Service (SCS) or Agricultural Research Service (ARS) programs, against 216 attributed to United States U.S. Army Corps of Engineers (USACE), 65 to the U.S. Forest Service (USFS), 45 to the USGS, 42 to Tennessee Valley Authority (TVA), and 41 to U.S. Bureau of Reclamation (USBR), with the remaining 203 held by other or unrecorded owners (Table 2).

Table 2. Summary statistics for the initial RESSED dataset before any selection or filtration of survey records

Category	Metric	Value
Dataset Scope	Survey records in the RESSED master table	6,617 (1,823 reservoirs, 45 states)
	Records by pool designation (T / S / A / G / none)	5,559 / 996 / 39 / 7 / 16
	T records with an assumed capacity of zero (removed)	734
	Reservoirs with an NID identifier, NID storage, height, and completion year	735 (2,159 records)
Ownership	SCS, NRCS, and ARS watershed structures	1,211 reservoirs
	USACE / TVA / USBR / USGS / USFS	216 / 42 / 41 / 45 / 65
	Other or unattributed	203

The analyzed RESSED database contains 6,617 survey records for 1,823 reservoirs across 45 states. Records were identified by a single-letter designation, listed in the RESSED documentation without further definition, as follows: T (5,559 records), S (996), A (39), G (7), and 16 undesignated records. The first T capacity (T0) equaled the sum of the RSED02 pool capacities within 1% at 1,473 of 1,546 reservoirs. The first S capacity matched the lowest listed pool at 192 of 231 multi-pool reservoirs, and that pool was the inactive pool in 143 of these. Survey records labeled T, identified as the total-pool capacity, were used in the subsequent filtering steps.

In this dataset, 734 records reported a capacity of zero and were removed. Of the 1,569 reservoirs, 1,555 (99.1%) held at least two surveys. The median T0 is 240 ac-ft with a maximum of 32,471,000 ac-ft, and the median drainage area is 2.55 sq mi. Survey dates spanned 1755 to 1997, and 4,338 of the 4,824 dated records (90%) fall between 1930 and 1979. Consecutive surveys at the same reservoir form 3,255 survey pairs, with a median interval of 5.0 years between surveys. Of these intervals, 583 were shorter than one year and 68 exceed 50 years. Reported capacities decreased in 2,368 pairs, stayed unchanged in 721, and increased in 166. Since sedimentation is associated with capacity loss; the increases are attributed to

sediment removal, structural modification, or revised survey computation. These results are summarized in Table 3.

The benchmark cohort was then derived by first restricting records to surveys with an NID identifier, NID storage, dam height, and completion year (2,159 records at 735 reservoirs), and surveys from one reservoir in Puerto Rico was excluded to limit the cohort to the contiguous United States. Where two or more surveys of a reservoir fell in the same calendar year, only the earliest was kept, which removed 25 records. Surveys dated before the NID completion year were then dropped (292 records), and the 54 reservoirs left without a survey were excluded. After reservoirs with fewer than two surveys were removed, 1,717 records at 557 reservoirs remained.

In the remaining three steps, whole reservoirs were retained or excluded. RESSED's reference initial capacity was defined as each reservoir's first T survey dated within five years after the NID completion year, and the 60 reservoirs without one were excluded. Where several RESSED reservoirs shared one NID identifier, only the reservoir with the RESSED reference initial capacity closest to NID storage was kept, which excluded 8 more reservoirs. Reservoirs with any capacity increase between consecutive surveys were then removed (45 reservoirs), so only capacity-loss sequences remain in the 444 reservoirs carried forward.

Table 3. Summary statistics for the T-designated survey working dataset

Category	Metric	Value
Survey Depth	Surveys per reservoir (mean/median/max)	3.1 / 2 / 31
	Reservoirs with at least two surveys	1,555 (99.1%)
	Consecutive survey pairs available	3,255
Temporal Coverage	Earliest and latest survey dates	1755 – 1997
	Peak survey decade	1960s (1,261 records)
	Interval between consecutive surveys (median)	5.0 years
	Intervals less than 1 year	583
	Intervals longer than 50 years	68
Capacity change	Pairs with decrease / no change / increase	2,368 / 721 / 166
Variable Ranges	Initial reported capacity	>0 – 32,471,000 ac-ft (median 240)
	Surveyed capacity	>0 – 32,471,000 ac-ft (median 156)
	Contributing drainage area	0.008 – 171,470 sq mi (median 2.55)
	Total storage loss, last survey vs. initial	median 8.5%
Ownership	SCS, NRCS, and ARS watershed structures	1,103 reservoirs

	USACE / TVA / USBR / USGS / USFS	118 / 29 / 34 / 44 / 55
	Other or unattributed	186
Climatic regime	Cold and very cold	670 reservoirs
	Mixed-humid / hot-humid	532 / 93
	Hot-dry / mixed-dry / marine	188 / 38 / 45
	Not classified	3

The comparison between initial NID storage and initial RESSED reference capacity was the most restrictive step. NID storage corresponds to normal or maximum storage, and it exceeded the initial RESSED reference capacity by more than 10% at 339 of the 444 reservoirs and was lower than 10% for a further 27 reservoirs. The 78 reservoirs within 10% were retained (200 records in 27 states).

A preliminary implementation of the WebApp enabled the identification of reservoirs for which the delineated drainage basins were inconsistent with the reported NID drainage areas, as well as those with drainage areas too small to support reliable geospatial data derivation. Accordingly, 24 reservoirs were excluded at this preliminary stage of the WebApp application because neither the NHDPlus nor the Merit-hydro watershed delineation areas were within 10% of the NID reported drainage area. An additional four reservoirs were excluded because their basins were too small to allow hydraulic length, channel slope, or curve number to be reliably derived from the input grids. The final benchmark dataset used for the WebApp validation consisted of 50 reservoirs and 135 survey records across 18 states. Validation results for three of these states are presented in the Regional Validation Cases section (Table 4).

Table 4. Final dataset size with reservoir and survey count by state. Validation results for California, Ohio and Tennessee are presented in the subsequent section.

State	Reservoirs	Surveys
CA	***14***	***33***
OH	***6***	***15***
TN	***5***	***17***
NC	3	14
KY	3	9
Other (13 states)	19	47

4.2.2. Regional Validation Cases

The predictive capabilities of the application were demonstrated through three regional case studies spanning California, Ohio and Tennessee. Together these cover 25 reservoirs across widely different hydrologic and geomorphic settings, evaluated against field survey measurements. The locations were selected to represent the states with the highest available survey count from our benchmarking dataset, as well as representing a range of reservoir sizes, climatic regimes, and agency types. Examples of the analysis outputs highlighted within the study areas are shown in Figures 8 through 11.

California: The state of California contributed the largest observational record of the three states (Figure 8). The predicted time series for 14 reservoirs were benchmarked against 33 observed survey points (Table 5), with NID storage ranging from 1,500 ac-ft (Matanzas Creek) to 1,091,700 ac-ft (Pine Flat Dam) and completion years from 1900 to 1963. The state average MAPE was 5.1% (median 6.2%) and the PBIAS was +0.6%. The state PBIAS was close to zero because the reservoir PBIAS values in either direction cancelled out.

At seven reservoirs, the error mainly arose from the initial offset. NID storage was 6.0% to 8.8% above the first survey at Pine Flat Dam, Upper Bear, East Park, Highland Creek and Elmer J. Chesbro, and 5.7% and 2.4% below it at Pardee and Chatsworth. At each of these, the PBIAS had the same sign as the initial offset and was within 1.2 percentage points of it, and the MAPE was close to the PBIAS in magnitude. The error therefore stayed close to the initial offset throughout the record, and the predicted rate of loss was close to the measured rate.

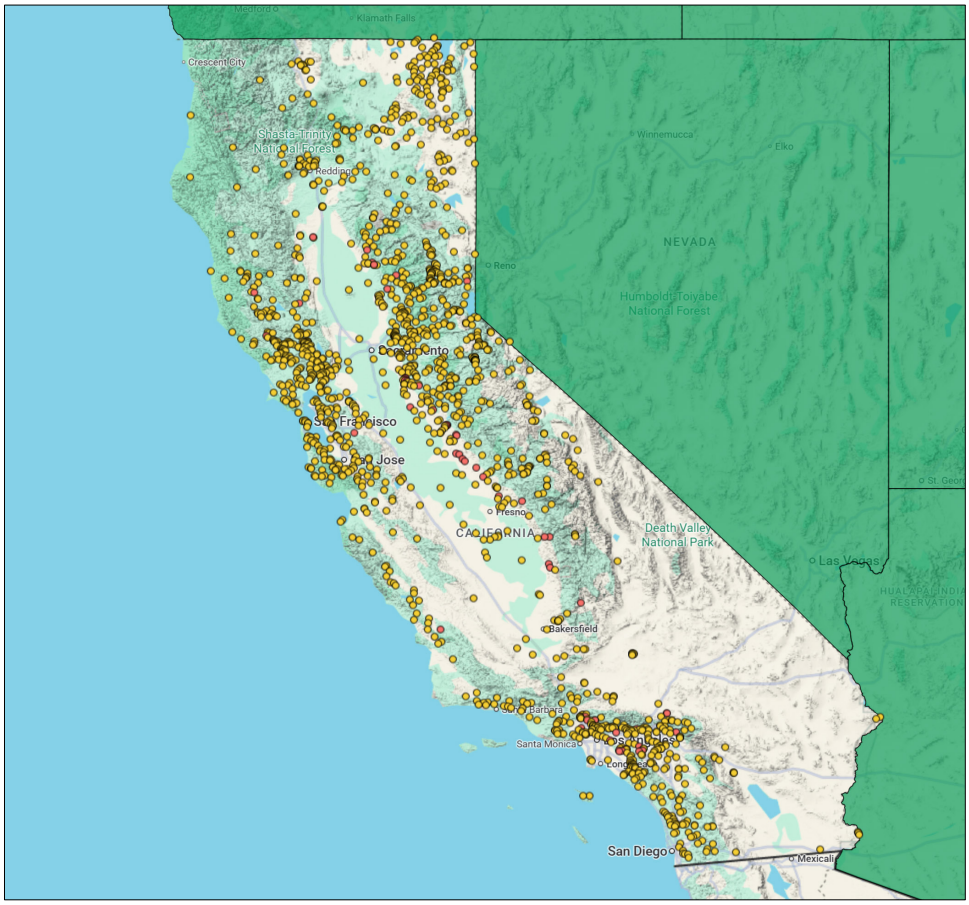


Figure 8. Distribution of all dams in the state of California from the National Inventory of Dams. Red markers indicate a USACE owned reservoir and yellow indicates all other reservoirs. For the case study, we chose selected reservoirs with good data coverage.

Bouquet Canyon, Fairmont and Matanzas Creek started within 0.3% initial offset and had the lowest errors in the state. Milliken and Bradbury started within 1.0%, but their higher errors came from the predicted rate of loss. At Milliken, the PBIAS (−3.3%) was larger in magnitude than the initial offset (−1.0%), so the model over-predicted loss. At Bradbury, the PBIAS (−0.1%) was close to zero, but the MAPE was 4.0%, because errors in opposite directions.

Most of the measured losses occurred early in the record, while the predicted loss increased later. The model therefore under-predicted loss at the earlier surveys and over-predicted it by the last survey.

Railroad Canyon had the highest MAPE in the state (9.7%). NID storage was 5.2% below its first survey, and the PBIAS (−9.6%) was larger in magnitude, so the model over-predicted loss on top of the initial offset. Railroad Canyon also had the largest drainage area relative to storage in the state. Juncal had the most surveys in the state (5). NID storage was 9.1% below its first survey, but the PBIAS (−5.5%) was smaller in magnitude than this offset. The error therefore decreased over the record, which means the model under-predicted loss.

Table 5. Results summary for the case study for the state of California.

Reservoir	NID ID	Year	NID Storage (ac-ft)	RESSED Init Survey (ac-ft)	Initial Offset	Surveys	MAPE	PBIAS
Juncal	CA00211	1930	6,140	6,754	−9.1%	5	6.4%	−5.5%
Pine Flat Dam	CA10112	1954	1,091,700	1,013,290	+7.7%	3	7.9%	+7.9%
Bradbury	CA10136	1953	206,900	204,874	+1.0%	3	4.0%	−0.1%
Railroad Canyon	CA00765	1928	11,586	12,218	−5.2%	2	9.7%	−9.6%
Bouquet Canyon	CA00088	1934	36,505	36,500	0.0%	2	0.1%	+0.1%
Chatsworth	CA00067	1918	9,886	10,125	−2.4%	2	2.9%	−2.8%
Fairmont	CA00071	1912	7,507	7,487	+0.3%	2	0.8%	−0.7%
Pardee	CA00164	1929	198,000	210,000	−5.7%	2	6.2%	−6.2%
Upper Bear	CA00379	1900	7,306	6,712	+8.8%	2	7.8%	+7.8%
East Park	CA10145	1910	54,300	50,900	+6.7%	2	7.9%	+7.9%
Milliken	CA00102	1924	1,980	2,000	−1.0%	2	3.3%	−3.3%
Highland Creek	CA00828	1962	3,500	3,235	+8.2%	2	7.5%	+7.5%
Matanzas Creek	CA00794	1963	1,500	1,500	0.0%	2	1.2%	−1.2%
Elmer J. Chesbro	CA00806	1955	8,086	7,630	+6.0%	2	6.2%	+6.2%

Ohio: Ohio (Figure 9) had the most accurate results of the three states. Predicted time series for 6 reservoirs were benchmarked against 15 survey points (Table 6). NID storage ranged from 11,380 ac-ft (West Fork of Mill Creek Dam) to 132,000 ac-ft (Delaware Dam), and completion years from 1936 to 1952. The state MAPE was 0.7% (median 0.5%) and the PBIAS was +0.4%. Unlike some of the reservoirs in other states, NID storage agreed with the first survey at every Ohio reservoir. The errors therefore came from the predicted rate of loss alone. Delaware Dam, Pleasant Hill Dam and Atwood Dam had a MAPE of 0.1%.

At the three reservoirs with larger errors, the PBIAS was close to the MAPE in magnitude, so the model erred in the same direction at each survey. The model under-predicted loss at Charles Mill Dam (MAPE 2.0%, PBIAS +1.9%) and West Fork of Mill Creek Dam (1.2%, +1.2%), and over-predicted it at Tom Jenkins Dam (0.9%, −0.9%). Charles Mill Dam and West Fork of Mill Creek Dam had the most surveys in the state (4 and 3) and the largest errors.

Table 6. Results summary for the case study for the state of Ohio.

Reservoir	NID ID	Year	NID Storage (ac-ft)	RESSED Init Survey (ac-ft)	Initial Offset	Surveys	MAPE	PBIAS
Charles Mill Dam	OH00020	1936	88,000	88,000	0.0%	4	2.0%	+1.9%
West Fork of Mill Creek Dam	OH00029	1952	11,380	11,376	0.0%	3	1.2%	+1.2%
Delaware Dam	OH00015	1951	132,000	132,000	0.0%	2	0.1%	−0.1%
Pleasant Hill Dam	OH00001	1937	87,700	87,700	0.0%	2	0.1%	+0.1%
Atwood Dam	OH00006	1936	49,700	49,700	0.0%	2	0.1%	+0.0%
Tom Jenkins Dam	OH00018	1950	26,900	26,910	0.0%	2	0.9%	−0.9%

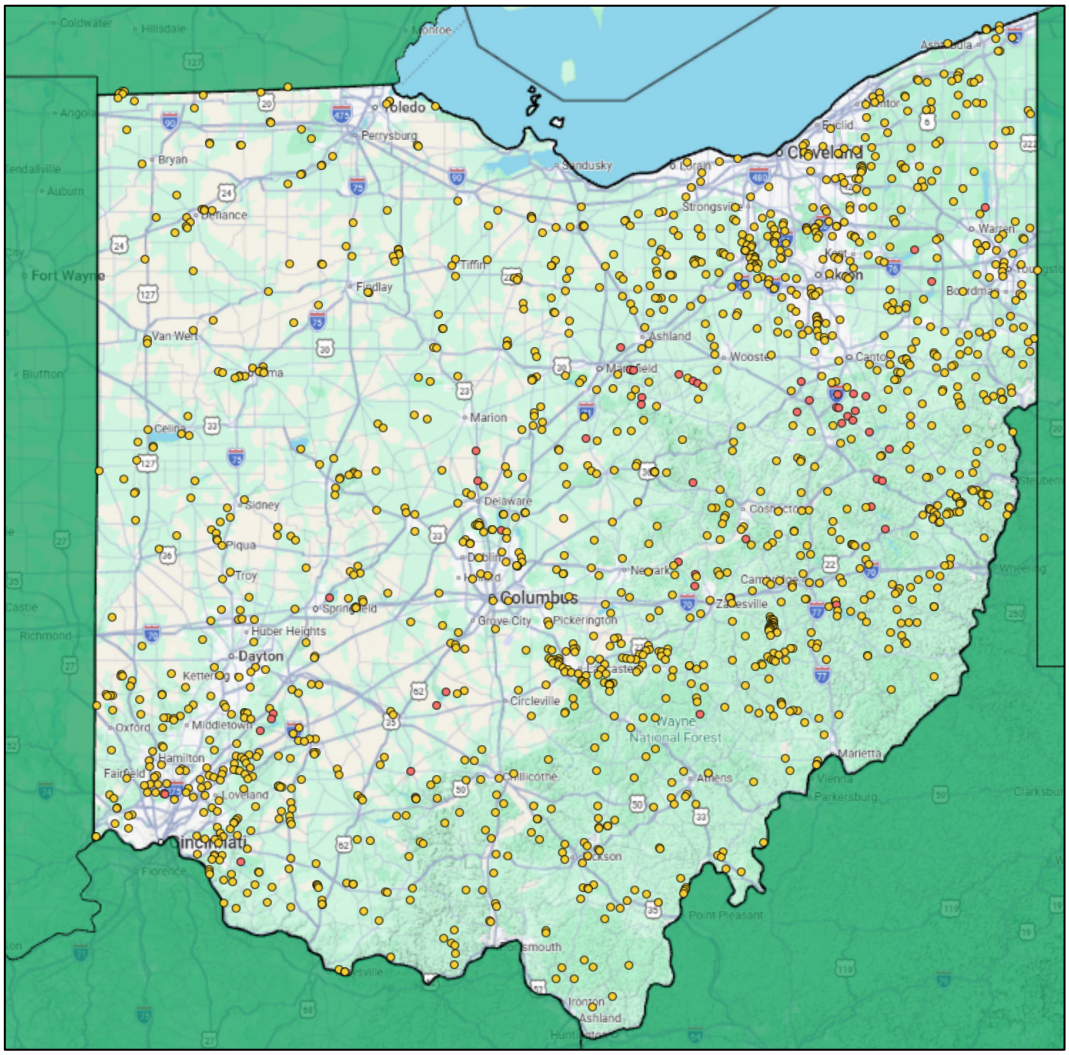


Figure 9. Distribution of all dams in the state of Ohio from the National Inventory of Dams. Red markers indicate a USACE-owned reservoir and yellow indicates all other reservoirs. For the case study, we chose reservoirs with good data coverage.

Tennessee: Tennessee had some of the largest reservoirs of the three states (Figure 10). Predicted time series for 5 reservoirs were benchmarked against 17 survey points (Table 7). NID storage ranged from 216,147 ac-ft (Boone Dam) to 1,706,000 ac-ft (Dale Hollow Dam),

and completion years from 1941 to 1973. NID lists all five as federal reservoirs. The state MAPE was 4.2% (median 1.0%) and the PBIAS was +4.0%.

Cherokee Dam (MAPE 9.1%, PBIAS +9.1%) and Boone Dam (9.5%, +9.5%) had the largest errors in the state. At both, NID storage was well above the first survey, with initial offsets of +9.0% and +9.9%. The PBIAS was within 0.4 percentage points of the initial offset and equal to the MAPE, so the error stayed close to the initial offset throughout the record. Almost all the errors at these two reservoirs came from the initial offset, and little from the predicted rate of loss. Cherokee Dam had the most surveys in the state (6). At Boone Dam, the PBIAS was slightly smaller than the initial offset, so the model slightly over-predicted loss.

At the other three reservoirs the initial offset was zero and the PBIAS equaled the MAPE in magnitude at all three, so the model carried in the same direction at every survey. The model under-predicted loss at Cordell Hull Lock and Dam (MAPE 1.0%, PBIAS +1.0%) and J. Percy Priest Dam (0.8%, +0.8%). Dale Hollow Dam (0.4%, −0.4%) was the only reservoir in the state with a negative PBIAS, where the model slightly over-predicted loss.

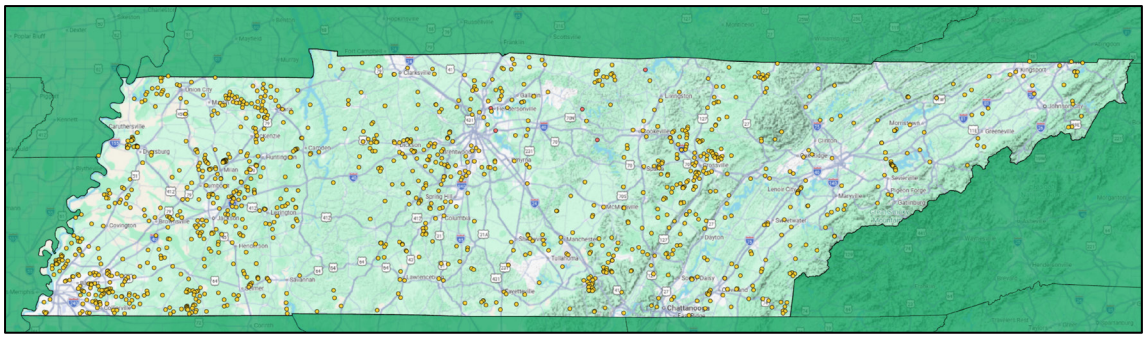


Figure 10. Distribution of all dams in Tennessee from the National Inventory of Dams. Red markers indicate a USACE owned reservoir and yellow indicates all other reservoirs. For the case study, we chose selected reservoirs with varying size and coverage.

Table 7. Results summary for the case study for Tennessee

Reservoir	NID ID	Year	NID Storage (ac-ft)	RESSED Init Survey (ac-ft)	Initial Offset	Surveys	MAPE	PBIAS
Cherokee Dam	TN08903	1941	1,699,431	1,559,570	+9.0%	6	9.1%	+9.1%
Cordell Hull Lock and Dam	TN15901	1973	310,900	310,900	0.0%	3	1.0%	+1.0%
J. Percy Priest Dam	TN03701	1967	652,000	652,000	0.0%	3	0.8%	+0.8%
Boone Dam	TN16306	1952	216,147	196,668	+9.9%	3	9.5%	+9.5%
Dale Hollow Dam	TN02702	1943	1,706,000	1,706,000	0.0%	2	0.4%	−0.4%

4.2.3. Summary of the Findings

Across the 25 reservoirs, the mean MAPE was 3.9% and the median was 2.9%. Twenty-two of the 25 fell below 8%, and 11 fell below 1.5%. Comparing the initial offset with the PBIAS and MAPE separated the errors into three groups. The first group consisted of the 14 reservoirs where NID storage agreed with the first survey to within 1.0%: six in Ohio, three in Tennessee and five in California. Their MAPE ranged from 0.1% to 4.0% (mean 1.1%). Because these reservoirs started with almost no offset, their errors came from the predicted rate of loss. The model under-predicted loss at Charles Mill Dam, West Fork of Mill Creek Dam, Cordell Hull

Lock and Dam and J. Percy Priest Dam, and over-predicted it at Milliken, Tom Jenkins Dam and Dale Hollow Dam. At Bradbury, the model under-predicted loss at the earlier surveys and over-predicted it by the last survey.

The second group consisted of the nine reservoirs where the initial offset was larger than 1.0% and within 1.2% of the PBIAS, for example Cherokee Dam (offset +9.0%, PBIAS +9.1%) and Boone Dam (+9.9%, +9.5%). At each of these, the MAPE was about the same size as the PBIAS, so the error stayed close to the initial offset throughout the record. The predicted rate of loss was close to the measured rate, and the error came from the difference between NID storage and the first survey. This group had a mean MAPE of 7.4% and included two of the three reservoirs with a MAPE above 8%.

The third group consisted of the two reservoirs where the initial offset was large but the PBIAS departed from it, because the predicted rate of loss also differed from the measured rate. At Railroad Canyon, the PBIAS (−9.6%) was larger in magnitude than the offset (−5.2%), so the model over-predicted loss on top of the offset. This gave the highest MAPE in the evaluation (9.7%; Figure 11). Railroad Canyon also had the largest drainage area relative to storage in California. At Juncal, the PBIAS (−5.5%) was smaller in magnitude than the offset (−9.1%), so the model under-predicted loss and the error decreased over the record.

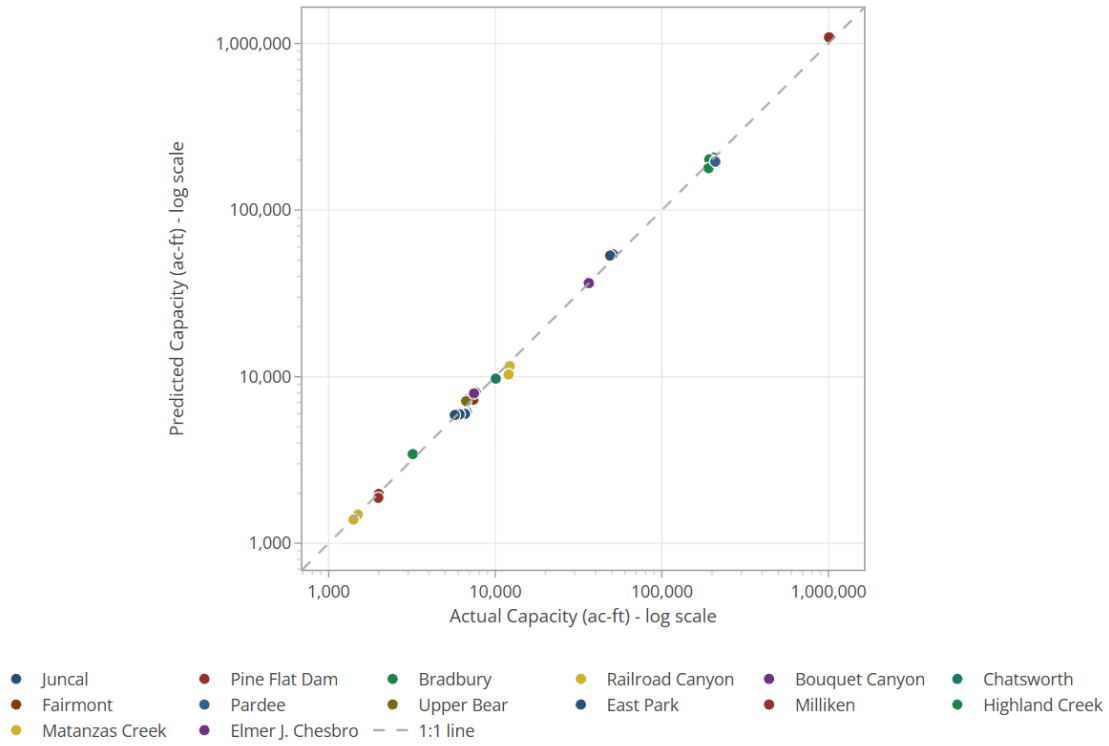


Figure 11. Log-log plot of all the surveys for California on a log-log plot. California has the widest storage span in the evaluation, from 1,500 to more than 1 million ac-ft. Most points lie close to the 1:1 line. The one exception is Railroad Canyon, whose 1939 survey is the furthest point from the center.

5. Discussions

This study presents a scalable framework for assessing reservoir sedimentation at the national level using sparse and heterogeneous observational data. By reformulating sedimentation as an

interval-based capacity change problem, the approach aligns prediction targets with available survey data and reduces reliance on continuous bathymetric records. The resulting framework supports consistent estimation of long-term storage decline across reservoirs with widely varying ages, sizes, and survey histories. The demonstrated performance for large federal reservoirs shows that meaningful sedimentation signals can be extracted from limited data when models are structured to reflect observational constraints.

Approximately 90% of RESSED survey labeled as were conducted between 1930 and 1979, with survey activity peaked in the 1960s with 1,261 records. This coincides with the era of major federal dam construction and the establishment of systematic sedimentation monitoring programs (Ackerman et al., 2009). The benchmark dataset therefore tests the model against capacity loss in the decades after construction, and few surveys exist for reservoirs completed after about 1980 or for recent decades. The record is also dominated by small SCS watershed structures, but most of these did not pass the filtering steps. As a result, the validation describes the model's performance for medium and large reservoirs better than for the small structures that make up most of RESSED.

The comparison between NID storage and the initial RESSED surveyed capacity was the most restrictive step in building the benchmark dataset and might explain some of the validation error. NID reports normal or maximum storage, while the T surveys report capacity up to the flood control pool, so the two sources might sometimes describe different pools. Where NID storage agreed with the first survey, errors were small. Where it did not, the error stayed close to the initial offset throughout the record, which shows that the model reproduced the measured rate of loss but started from a different capacity. Large errors were less common and occurred at reservoirs with unusual conditions, such as Railroad Canyon, which has a high drainage area relative to its storage.

The integration of machine learning with automated GIS workflows is central to the framework’s scalability. Automated watershed delineation, feature extraction, and data synchronization enable reproducible inference across thousands of reservoirs without site-specific calibration. Machine learning provides the capacity to learn nonlinear relationships among climatic forcing, basin characteristics, and upstream infrastructure, while GIS automation ensures that these predictors can be generated consistently at national scale.

The framework is intended to support strategic planning on a regional scale. Predicted capacity trajectories enable agencies to identify reservoirs experiencing relatively rapid storage loss and to prioritize sites for additional monitoring, field surveys, or feasibility assessments. At regional and national scales, the results provide a consistent basis for comparing sedimentation risk across large portfolios of reservoirs with differing management objectives. Many U.S. reservoirs lack recent sedimentation surveys or any documented measurements beyond initial design storage. For these systems, the framework provides first-order estimates of capacity decline that would otherwise be unavailable. While uncertainty remains inherent for unmonitored sites, the ability to generate comparable predictions across data-sparse regions addresses a key gap in current national sedimentation management practices.

5.1. Limitations

Despite its demonstrated utility at national scale, the proposed framework evaluation is subject to several limitations arising from data availability, structural uncertainty in national

inventories, scale effects, and methodological assumptions inherent to large-domain sedimentation assessment. Model verification relies on reservoir sedimentation surveys archived in RESSED, which represent a small and non-uniform subset of U.S. reservoirs. Even among federally managed reservoirs, survey frequency is irregular and often separated by decades. This temporal sparsity limits the model's exposure to short-term variability and forces reliance on long-interval averages. The quality-control workflow improves internal consistency but cannot recover information absent from the underlying record. As a result, predictions reflect long-term mean behavior more reliably than episodic or event-driven sedimentation processes.

A fundamental limitation arises from inconsistencies between reported reservoir capacities across federal datasets. Modelled trajectories are anchored to NID normal or maximum storage values, whereas validation surveys drawn from RESSED may reference differing operational definitions, or survey conventions. Survey records originated from multiple agencies and span long time periods, introducing unavoidable inconsistencies in measurement conventions and reference conditions. Additionally, different conventions in measuring pool and gross capacities introduce further complications, and that data needed to be aggregated and matched to NID initial capacities for use in analysis. Survey frequency is irregular even among federally managed structures, and the compiled record carries a median interval of five years between consecutive measurements alongside individual gaps exceeding fifty.

This temporal sparsity limits the resolution at which short-term variability can be observed and confines verification to long-interval averages. The curation workflow improves internal consistency but cannot recover information absent from the underlying record. Predictions therefore describe long-term mean behavior more reliably than episodic or event-driven sedimentation processes. Moreover, the tool described herein, and the implementation of the DNN framework correctly captures the downward trend when comparing slope tendencies across these multiple domains. A focus on relative capacity change between consecutive surveys would limit sensitivity to such inconsistencies and supports comparative analysis across reservoirs with differing survey histories.

Model performance also degrades as reservoirs offset from the size, hydraulic context, and management characteristics represented in the training data. Very small reservoirs, including many NRCS watershed structures, exhibit higher relative errors. These systems are strongly influenced by localized controls such as small-scale channel dynamics, maintenance interventions, and short-duration storm events, that are not captured by basin-averaged predictors.

Climatic and upstream infrastructure variables are summarized over 15-year intervals to match survey resolution and promote temporal stationarity in the learning problem. This aggregation limits sensitivity to extreme events, such as individual floods, wildfire-driven erosion pulses, or rapid upstream development, that can dominate sediment delivery in certain settings. While the chosen interval length provides stability for national application, it introduces uncertainty in environments where sedimentation is controlled by highly episodic processes. The predictor set does not explicitly include sediment grain size distributions, reservoir operating rules, flushing activities, or dredging histories beyond coarse anomaly

filtering. These processes influence sediment trapping efficiency and deposition patterns but are unavailable at national scale in consistent form.

Consequently, the framework captures emergent sedimentation behavior driven by climatic, geomorphic, and infrastructural proxies as well as historical upstream dam inventories which do not account for non-stationary future climate conditions or altered watershed behavior due to land use change beyond what is embedded in the training data. Given these constraints, model outputs are best used for comparative assessment, prioritization, and risk screening across large reservoir portfolios. The framework is not intended to replace site-specific sediment transport modelling or detailed engineering studies, particularly where operational decisions or structural modifications are under consideration.

6. Conclusions

This study developed and demonstrated an end-to-end, data-driven framework for assessing reservoir sedimentation at national scale under conditions of sparse and heterogeneous data availability. The framework integrates historical sedimentation surveys, automated data quality control, geospatial feature extraction, interval-based machine learning, and web-based deployment to generate consistent reservoir capacity trajectories across the contiguous United States. By reformulating sedimentation prediction as an interval-based capacity change problem, the approach aligns directly with the temporal structure of available survey records and supports cumulative reconstruction of reservoir storage through time. Results show that this formulation produces stable and interpretable trajectories for medium and large federal reservoirs, where predicted capacity loss aligns closely with observed survey measurements. Performance degrades predictably outside the training domain, particularly for very small impoundments and highly episodic hydrologic regimes, defining a clear range of applicability for the method.

The study highlights the importance of scalable, data-driven sedimentation assessment for supporting national reservoir management. In the absence of comprehensive monitoring, the framework provides a consistent basis for comparing sedimentation risk across large inventories of unmonitored or data-sparse reservoirs. While not a substitute for site-specific physical modelling or field investigation, the system supports strategic screening, prioritization, and long-term planning at regional and institutional levels. Deployment through a web-based decision-support application demonstrates how predictive models, geospatial automation, and national datasets can be operationalized into accessible tools for practitioners. By exposing intermediate data products alongside model outputs, the system promotes transparency and informed interpretation of sedimentation estimates. This project demonstrates a practical pathway for translating sparse national datasets into actionable insight for long-term water resources management.

6.1. Future Research

The presented framework is well suited to guide targeted application of physically based sediment transport models. Data-driven predictions can be used to identify reservoirs exhibiting rapid capacity decline or high uncertainty, narrowing the set of sites where detailed process-based modelling is most impactful. At these locations, physically based models can better resolve grain size effects, density currents, and reservoir operation impacts that are not

represented in national datasets. Feedback from these localized studies may also inform refinement of predictor selection or interval structuring in the data-driven framework.

Future work will prioritize reconciliation of reference storage definitions across national inventories and sedimentation archives. Aligning NID-reported capacities with survey-based pool definitions or incorporating survey-derived baseline adjustments would reduce structural offsets in reconstructed trajectories. Advances in metadata standardization and automated detection of reference inconsistencies would directly improve inference reliability without increasing model complexity.

The underlying architecture of modern reservoir information systems is well positioned to evolve alongside emerging advances in domain-adapted large language models and AI-assisted computing. Recent developments in hydrology-specific benchmarking and model evaluation frameworks highlight the growing potential for integrating natural language interfaces with complex geoprocessing workflows, enabling more intuitive interaction with large-scale environmental data (Kizilkaya et al., 2025). In parallel, advances in AI-assisted and voice-enabled computing point toward more accessible approaches for querying spatial datasets and executing analytical pipelines, reducing technical barriers for a broader range of users (Erazo Ramirez & Demir, 2026). These trends, coupled with ongoing efforts in experiential and AI-integrated training environments, suggest a clear trajectory toward more interactive, scalable, and user-centric hydroinformatics systems (Sajja et al., 2024; 2026).

As new sedimentation surveys and infrastructure records become available, future systems could support incremental updating of predictions and periodic model retraining. Incorporating update workflows would allow the framework to transition from a retrospective assessment tool toward an operational support system that evolves with the observational record. Such capabilities would be particularly valuable for agencies managing long-term sedimentation under changing watershed and infrastructure conditions.

7. Acknowledgements

This research was supported by the U.S. Army Corps of Engineers (Federal Award Identification Number: W912HZ-23-2-0040) and the WATER Institute at Saint Louis University

8. Declaration of AI Assisted Technologies

During the preparation of this work the authors used ChatGPT and Claude to develop the software herein described and improve readability throughout the manuscript. After using this tool/service, the authors reviewed and edited the content as needed and take full responsibility for the content of the publication.

9. CRediT Statement

Moiyyad Sufi: Data curation, Formal analysis, Investigation, Methodology, Software, Visualization, Writing – original draft. **Alejandra Botero-Acosta:** Data curation, Formal analysis, Investigation, Methodology, Software, Visualization, Writing – review & editing. **Carlos Erazo Ramirez:** Investigation, Methodology, Writing – original draft. **Amanda L. Cox:** Conceptualization, Funding acquisition, Methodology, Project Administration, Supervision, Writing – review & editing. **Paul Boyd:** Methodology, Writing – review &

editing. **Marian Muste:** Conceptualization, Funding acquisition, Methodology, Writing – review & editing. **Ibrahim Demir:** Conceptualization, Funding acquisition, Methodology, Project Administration, Supervision, Writing – review & editing.

10. References

Ackerman, K. V., Mixon, D. M., Sundquist, E. T., Stallard, R. F., Schwarz, G. E., & Stewart, D. W. (2009). RESIS-II: An updated version of the original reservoir sedimentation survey information system (RESIS) database. *Data Series*. https://doi.org/10.3133/ds434

Advisory Committee on Water Information, Subcommittee on Sedimentation. (2009, March). *Reservoir Sedimentation Database*. Retrieved July 31, 2026, from https://water.usgs.gov/osw/ressed/index.html

Alabbad, Y., Mount, J., Campbell, A. M., & Demir, I. (2024). A web-based decision support framework for optimizing road network accessibility and emergency facility allocation during flooding. *Urban Informatics*, *3*(1). https://doi.org/10.1007/s44212-024-00040-0

Alfieri, L., Pappenberger, F., Wetterhall, F., Haiden, T., Richardson, D., & Salamon, P. (2014). Evaluation of ensemble streamflow predictions in Europe. *Journal of Hydrology*, *517*, 913-922. https://doi.org/10.1016/j.jhydrol.2014.06.035

Annandale, G. W., Morris, G. L., & Karki, P. (2016). *Extending the life of reservoirs: Sustainable sediment management for dams and run-of-river hydropower*. Directions in Development. World Bank. https://doi.org/10.1596/978-1-4648-0838-8

Baydaroğlu, Ö., Yeşilköy, S., Sermet, Y., & Demir, I. (2023). A comprehensive review of Ontologies in the hydrology towards guiding next generation artificial intelligence applications. *Journal of Environmental Informatics*. https://doi.org/10.3808/jei.202300500

Beck, M.B., Jiang, F., Shi, F., Walker, R.V., Osidele, O.O., Lin, Z., Demir, I. and Hall, J.W., 2010, March. Re-engineering cities as forces for good in the environment. In *Proceedings of the institution of civil engineers-engineering sustainability* (Vol. 163, No. 1, pp. 31-46). Thomas Telford Ltd.

Botero-Acosta, A., Cox, A. L., Sagan, V., Demir, I., Muste, M., Boyd, P., & Pathak, C. (2024). Multivariate analysis and anomaly detection of a US reservoir sedimentation data set. *Journal of Hydrologic Engineering*, *29*(5). https://doi.org/10.1061/jhyeff.heeng-6206

Brune, G. M. (1953), *Trap efficiency of reservoirs*, *Eos Trans. AGU*, 34(3), 407–418, https://doi.org/10.1029/TR034i003p00407.

Chegini, T., Li, H., & Leung, L. R. (2021). HyRiver: Hydroclimate Data Retriever. Journal of Open Source Software, 6(66), 1–3. https://doi.org/10.21105/joss.03175

Churchill, M. A. (1948). Discussion of analysis and use of reservoir sedimentation data. Proc. of Federal Interagency Sedimentation Conference, Denver, Colorado, United States Bureau of Reclamation, p.139-140

Cox, A. L., Meyer, D., Botero-Acosta, A., Sagan, V., Demir, I., Muste, M., Boyd, P., & Pathak, C. (2024). Estimating reservoir sedimentation using machine learning. *Journal of Hydrologic Engineering*, *29*(4). https://doi.org/10.1061/jhyeff.heeng-6135

Dawson, C., Abrahart, R., & See, L. (2010). HydroTest: Further development of a web resource for the standardised assessment of hydrological models. *Environmental Modelling & Software*, *25*(11), 1481-1482. https://doi.org/10.1016/j.envsoft.2009.01.001

Demir, I., & Beck, M. B. (2009, April). GWIS: a prototype information system for Georgia watersheds. In *Georgia Water Resources Conference: Regional Water Management Opportunities, UGA, Athens, GA, US*.

Demiray, B. Z., Sit, M., Mermer, O., & Demir, I. (2024). Enhancing hydrological modeling with transformers: A case study for 24-h streamflow prediction. *Water Science & Technology*, *89*(9), 2326-2341. https://doi.org/10.2166/wst.2024.110

Ebert-Uphoff, I., Thompson, D.R., Demir, I., Gel, Y.R., Karpatne, A., Guereque, M., Kumar, V., Cabral-Cano, E. and Smyth, P., 2017, September. A vision for the development of benchmarks to bridge geoscience and data science. In *17th international workshop on climate informatics*.

El Bilali, A., Brouziyne, Y., Attar, O., Lamane, H., Hadri, A., & Taleb, A. (2024). Physics-informed machine learning algorithms for forecasting sediment yield: An analysis of physical consistency, sensitivity, and interpretability. *Environmental Science and Pollution Research*, *31*(34), 47237-47257. https://doi.org/10.1007/s11356-024-34245-2

EPA. (2022). NHDPlus (National Hydrography Dataset Plus). https://www.epa.gov/waterdata/nhdplus-national-hydrography-dataset-plus

Erazo Ramirez, C., & Demir, I. (2026). AI-assisted voice enabled computing framework for hydrological analysis. *Environmental Modelling & Software*, *197*, 106833. https://doi.org/10.1016/j.envsoft.2025.106833

Erazo Ramirez, C., Sermet, Y., & Demir, I. (2023). HydroLang markup language: Community-driven web components for hydrological analyses. *Journal of Hydroinformatics*, *25*(4), 1171-1187. https://doi.org/10.2166/hydro.2023.149

Ewing, G., Erazo Ramirez, C., Vaidya, A., & Demir, I. (2024). Client-side web-based model coupling using basic model interface for hydrology and water resources. *Journal of Hydroinformatics*, *26*(2), 494-502. https://doi.org/10.2166/hydro.2024.212

Fan, J. (1986). Turbid density currents in reservoirs. Water International, 11(3), 107–116. https://doi.org/10.1080/02508068608686404

García-Feal, O., González-Cao, J., Fernández-Nóvoa, D., Astray Dopazo, G., & Gómez-Gesteira, M. (2022). Comparison of machine learning techniques for reservoir outflow forecasting. *Natural Hazards and Earth System Sciences*, *22*(12), 3859-3874. https://doi.org/10.5194/nhess-22-3859-2022

Gibson, S., & Sánchez, A. (2020). *HEC-RAS sediment transport user's manual* (Version 6.0) [CPD-68]. U.S. Army Corps of Engineers, Institute for Water Resources, Hydrologic Engineering Center. https://www.hec.usace.army.mil/software/hec-ras/documentation/HEC-RAS_6.0_1D_Sediment_User_Manual.pdf

Graf, W. L., Wohl, E., Sinha, T., & Sabo, J. L. (2010). Sedimentation and sustainability of western American reservoirs. *Water Resources Research*, *46*(12). https://doi.org/10.1029/2009wr008836

Granata, F., Di Nunno, F., Najafzadeh, M., & Demir, I. (2022). A stacked machine learning algorithm for multi-step ahead prediction of soil moisture. *Hydrology*, *10*(1), 1.

Grill, G., Lehner, B., Thieme, M., Geenen, B., Tickner, D., Antonelli, F., Babu, S., Borrelli, P., Cheng, L., Crochetiere, H., Ehalt Macedo, H., Filgueiras, R., Goichot, M., Higgins, J., Hogan, Z., Lip, B., McClain, M. E., Meng, J., Mulligan, M., . . . Zarfl, C. (2019). Mapping the world's free-flowing rivers. *Nature*, *569*(7755), 215–221. https://doi.org/10.1038/s41586-019-1111-9

Gunderson, J. (2026, March 12). *Aging US dams pose rising safety risks – how can civil engineers help?* Civil Engineering Source, American Society of Civil Engineers. https://www.asce.org/publications-and-news/civil-engineering-source/article/2026/03/12/aging-us-dams-pose-rising-safety-risks-how-can-civil-engineers-help

Gupta, H. V., Sorooshian, S., & Yapo, P. O. (1999). Status of automatic calibration for hydrologic models: Comparison with multilevel expert calibration. *Journal of Hydrologic Engineering*, *4*(2), 135-143. https://doi.org/10.1061/(asce)1084-0699(1999)4:2(135)

Heberger, M. (2023). delineator.py: Fast, accurate watershed delineation using hybrid vector- and raster-based methods and data from MERIT-Hydro (v1.2). Zenodo. https://github.com/mheberger/delineator/tree/main

Hodson, T. O. (2022). Root-mean-square error (RMSE) or mean absolute error (MAE): When to use them or not. *Geoscientific Model Development*, *15*(14), 5481-5487. https://doi.org/10.5194/gmd-15-5481-2022

Hubbart S. & Ross L. (2026). The increasing demand and decreasing supply of water. The National Environmental Education Foundation (NEEF). https://www.neefusa.org/story/water/increasing-demand-and-decreasing-supply-water

Juracek, K. E. (2015). The aging of America's reservoirs: In-reservoir and downstream physical changes and habitat implications. *JAWRA Journal of the American Water Resources Association*, *51*(1), 168-184. https://doi.org/10.1111/jawr.12238

Kaynak, S., Kaynak, B., Mermer, O., & Demir, I. (2025). City-scale digital twin framework for flood impact analysis: Integrating urban infrastructure and real-time data analytics. *Urban Climate*, *64*, 102640. https://doi.org/10.1016/j.uclim.2025.102640

Kizilkaya, D., Sajja, R., Sermet, Y., & Demir, I. (2025). Toward HydroLLM: A benchmark dataset for hydrology-specific knowledge assessment for large language models. *Environmental Data Science*, *4*. https://doi.org/10.1017/eds.2025.10006

Kondolf, G. M., Gao, Y., Annandale, G. W., Morris, G. L., Jiang, E., Zhang, J., Cao, Y., Carling, P., Fu, K., Guo, Q., Hotchkiss, R., Peteuil, C., Sumi, T., Wang, H., Wang, Z., Wei, Z., Wu, B., Wu, C., & Yang, C. T. (2014). Sustainable sediment management in reservoirs and regulated rivers: Experiences from five continents. *Earth's Future*, *2*(5), 256-280. https://doi.org/10.1002/2013ef000184

Lin, P., Pan, M., Beck, H. E., Yang, Y., Yamazaki, D., Frasson, R., David, C. H., Durand, M., Pavelsky, T. M., & Allen, G. H. (2019). Global reconstruction of naturalized river flows at 2.94 million reaches. Water Resources Research, 55(8), 6499-6516.

Li, H., Tan, Z., Ma, H., Zhu, Z., Abeshu, G. W., Zhu, S., Cohen, S., Zhou, T., Xu, D., & Leung, L. R. (2022). A new large-scale suspended sediment model and its application over the United States. *Hydrology and Earth System Sciences*, *26*(3), 665-688. https://doi.org/10.5194/hess-26-665-2022

Li, Z., Duque, F. Q., Grout, T., Bates, B., & Demir, I. (2023). Comparative analysis of performance and mechanisms of flood inundation map generation using Height Above Nearest Drainage. *Environmental Modelling & Software*, *159*, Article 105565. https://doi.org/10.1016/j.envsoft.2022.105565

Minocha, S., & Hossain, F. (2025). GRILSS: Opening the gateway to global reservoir sedimentation data curation. *Earth System Science Data*, *17*(4), 1743-1759. https://doi.org/10.5194/essd-17-1743-2025

Minocha, S., Hossain, F., Zhao, J., & Istanbulluoglu, E. (2026). Reclaim: A globally scalable machine learning framework to predict reservoir sedimentation and capacity loss from satellite-based earth observations. *Environmental Modelling & Software*. https://doi.org/10.1016/j.envsoft.2026.107055

Morris, G. L., & Fan, J. (1998). Reservoir sedimentation handbook: Design and management of dams, reservoirs, and watersheds for sustainable use. McGraw Hill Professional.

Mouris, K., Schwindt, S., Pesci, M. H., Wieprecht, S., & Haun, S. (2023). An interdisciplinary model chain quantifies the footprint of global change on reservoir sedimentation. *Scientific Reports*, *13*(1). https://doi.org/10.1038/s41598-023-47501-1

Office of Habitat Conservation. (2026, January 9). *River habitat*. Retrieved August 3, 2026, from https://www.fisheries.noaa.gov/national/habitat-conservation/river-habitat

Palmieri, A., Shah, F., Annandale, G., & Dinar, A. (2003). Reservoir conservation volume I: the RESCON approach. *Washington, DC: World Bank*.

Perera, D., Smakhtin, V., Williams, S., North, T., & Curry, A. (2021). Ageing water storage infrastructure: An emerging global risk. *United Nations University Institute for Water, Environment and Health (UNU-INWEH)*. https://doi.org/10.53328/qsyl1281

Perera, D., Williams, S., & Smakhtin, V. (2022). Present and future losses of storage in large reservoirs due to sedimentation: A country-wise global assessment. *Sustainability*, *15*(1), 219. https://doi.org/10.3390/su15010219

Pinson, A., Baker, B., Boyd, P., Grandpre, R., White, K. D., & Jonas, M. (2016). *U.S. Army Corps of Engineers reservoir sedimentation in the context of climate change* (Civil Works Technical Report CWTS 2016-05). U.S. Army Corps of Engineers. https://cdm16021.contentdm.oclc.org/digital/collection/p266001coll1/id/5201

Podolak, C. J., & Doyle, M. W. (2015). Reservoir sedimentation and storage capacity in the United States: Management needs for the 21st century. *Journal of Hydraulic Engineering*, *141*(4). https://doi.org/10.1061/(asce)hy.1943-7900.0000999

Randle, T. J., Morris, G. L., Tullos, D. D., Weirich, F. H., Kondolf, G. M., Moriasi, D. N., Annandale, G. W., Fripp, J., Minear, J. T., & Wegner, D. L. (2021). Sustaining United States reservoir storage capacity: Need for a new paradigm. *Journal of Hydrology*, *602*, 126686. https://doi.org/10.1016/j.jhydrol.2021.126686

Sajja, R., Mermer, O., Sermet, Y., & Demir, I. (2026). Hydro3DJS: A modular web-based library for real-time 3D visualization of watershed dynamics and digital twin integration. *Environmental Modelling & Software*, *197*, 106853. https://doi.org/10.1016/j.envsoft.2025.106853

Sajja, R., Ramirez, C. E., Li, Z., Demiray, B. Z., Sermet, Y., & Demir, I. (2024). Integrating generative AI in Hackathons: Opportunities, challenges, and educational implications. *Big Data and Cognitive Computing*, *8*(12), 188. https://doi.org/10.3390/bdcc8120188

Schleiss, A. J., Franca, M. J., Juez, C., & De Cesare, G. (2016). Reservoir sedimentation. *Journal of Hydraulic Research*, *54*(6), 595–614. https://doi.org/10.1080/00221686.2016.1225320

Sermet, Y., Liang, C., Dey, S., Muste, M., Merwade, V., Cox, A. L., Minear, J. T., & Demir, I. (2025). River morphology information system: A web cyberinfrastructure for advancing river morphology research. *Environmental Modelling & Software*, *183*, 106222. https://doi.org/10.1016/j.envsoft.2024.106222

Shelley, J., & Boyd, P. (2025). Measured and projected loss of water storage in 162 USACE reservoirs due to sedimentation: 1938–2074. https://doi.org/10.21079/11681/50036

Shelley, J., Hotchkiss, R. H., Boyd, P., & Gibson, S. (2022). Discharging sediment downstream: Case studies in cost effective, environmentally acceptable reservoir sediment management in the United States. *Journal of Water Resources Planning and Management*, *148*(2). https://doi.org/10.1061/(asce)wr.1943-5452.0001494

Sohrabzadeh Anzani, H., Kantoush, S. A., & Nguyen, B. Q. (2026). Sediment management in reservoirs: A comprehensive review of processes, trapping efficiency, Flushing techniques, and bypass solutions. *Progress in Disaster Science*, *30*, 100556. https://doi.org/10.1016/j.pdisas.2026.100556

Steffen, L.J., 1996, A Reservoir Sedimentation Survey Information System—RESIS, in Proceedings of the Sixth Federal Interagency Sedimentation Conference, Las Vegas, NV, 1996: v. 1, p. I–29 to I–36. (Accessed online July 31, 2026, at https://water.usgs.gov/osw/ressed/references/steffen-1996.pdf.)

Sufi, M., Erazo Ramirez, C., & Demir, I. (2025). HydroLang FRAM: Web-based framework for comprehensive flood risk and mitigation assessment and communication. International Journal of Disaster Risk Reduction, 105735.

Swain, N. R., Christensen, S. D., Snow, A. D., Dolder, H., Espinoza-Dávalos, G., Goharian, E., Jones, N. L., Nelson, E. J., Ames, D. P., & Burian, S. J. (2016). A new open source platform for lowering the barrier for environmental web app development. *Environmental Modelling & Software, 85*, 11–26. https://doi.org/10.1016/j.envsoft.2016.08.003

Tullos, D., Nelson, P. A., Hotchkiss, R. H., & Wegner, D. (2021, April 14). *Sediment Mismanagement Puts Reservoirs and Ecosystems at Risk*. Eos. https://eos.org/opinions/sediment-mismanagement-puts-reservoirs-and-ecosystems-at-risk

U.S. Army Corps of Engineers. (2015). *Enhancing reservoir sedimentation information web Portal (RSI) - PROD v2.8 - Home*. Retrieved September 2, 2026, from https://cwbi-app.sec.usace.army.mil/ords/f?p=303:1::::::

U.S. Army Corps of Engineers. (2026). *Update Reservoir Sediment Information*. Retrieved September 2, 2026, from https://www.usace.army.mil/Missions/Infrastructure-and-Installation-Resilience/Climate-Preparedness-and-Resilience/Update-Reservoir-Sediment-Information/

U.S. Energy Information Administration. (2019, March). *Nonpowered dams can be converted to hydroelectric dams for electricity generation*. Today in Energy. https://www.eia.gov/todayinenergy/detail.php?id=39552

U.S. Forest Service. (2026). *Water facts*. U.S. Department of Agriculture. Retrieved September 2, 2026, from https://www.fs.usda.gov/managing-land/national-forests-grasslands/water-facts

Whelan, M., & Hotchkiss, R. (2024). A dwindling water supply caused by reservoir sedimentation troubles engineers. Civil Engineering Magazine.

Xu, H., Muste, M., & Demir, I. (2019). Web-based geospatial platform for the analysis and forecasting of sedimentation at culverts. Journal of Hydroinformatics, 21(6), 1064–1081.

Yamazaki, D., Ikeshima, D., Sosa, J., Bates, P. D., Allen, G. H., & Pavelsky, T. M. (2019). MERIT Hydro: A high-resolution global hydrography map based on latest topography dataset. Water Resources Research, 55(6), 5053-5073.

Yeşilköy, S., Baydaroğlu, Ö., Singh, N., Sermet, Y., & Demir, I. (2024). A contemporary systematic review of cyberinfrastructure systems and applications for flood and drought data analytics and communication. *Environmental Research Communications*, *6*(10), 102003.

USACE. (2021). *National Inventory of Dams*. Retrieved from https://nid.sec.usace.army.mil/#/